Title

Expression of CD40L by the ALVAC-Simian Immunodeficiency Virus Vector Abrogates T Cell Responses in Macaques.

Journal

Journal of Virology, 94(6)

ISSN

0022-538X

Authors

Silva de Castro, Isabela
Gordon, Shari N
Liu, Jun
et al.

Publication Date

2020-02-28

DOI

10.1128/jvi.01933-19

Peer reviewed

AMERICAN SOCIETY FOR MICROBIOLOGY | Journal of Virology®

VACCINES AND ANTIVIRAL AGENTS

Expression of CD40L by the ALVAC-Simian Immunodeficiency Virus Vector Abrogates T Cell Responses in Macaques

Isabela Silva de Castro,[a] Shari N. Gordon,[a] Jun Liu,[b,l] Massimiliano Bissa,[a] Katherine McKinnon,[c] Hung V. Trinh,[d,e] Melvin N. Doster,[a] Luca Schifanella,[a] Namal P. Liyanage,[a]* JinChao Cao,[b,l] Olivia Cheng,[b,l] Kathryn Foulds,[f] Mario Roederer,[f] Richard A. Koup,[f] Xiaoying Shen,[g] Georgia D. Tomaras,[g] David J. Venzon,[h] Donald N. Forthal,[i] Timothy Fouts,[j] David C. Montefiori,[g] Jim Tartaglia,[k] Mangala Rao,[d] Mario Ostrowski,[b,l] Genoveffa Franchini,[a] Monica Vaccari[a]

[a]Animal Models and Retroviral Vaccines Section, National Cancer Institute, National Institutes of Health, Bethesda, Maryland, USA
[b]Department of Medicine, University of Toronto, Toronto, Canada
[c]Vaccine Branch Flow Cytometry Core, National Cancer Institute, National Institutes of Health, Bethesda, Maryland, USA
[d]Henry M. Jackson Foundation for the Advancement of Military Medicine, Bethesda, Maryland, USA
[e]U.S. Military HIV Research Program, Walter Reed Army Institute of Research, Silver Spring, Maryland, USA
[f]Vaccine Research Center, National Institutes of Health, Bethesda, Maryland, USA
[g]Department of Surgery, Duke Human Vaccine Institute, Durham, North Carolina, USA
[h]Biostatistics and Data Management Section, National Cancer Institute, National Institutes of Health, Bethesda, Maryland, USA
[i]University of California, Irvine School of Medicine, Irvine, California, USA
[j]Advanced Bioscience Laboratories, Rockville, Maryland, USA
[k]Sanofi Pasteur, Swiftwater, Pennsylvania, USA
[l]Keenan Research Center, St. Michael's Hospital, Toronto, Canada

ABSTRACT Immunization with recombinant ALVAC/gp120 alum vaccine provided modest protection from human immunodeficiency virus type 1 (HIV-1) and simian immunodeficiency virus (SIV) acquisition in humans and macaques. Vaccine-mediated protection was associated with the elicitation of IgG against the envelope V2 loop and of envelope-specific $CD4^+$ T cell responses. We hypothesized that the simultaneous expression of the costimulatory molecule CD40L (CD154) by the ALVAC-HIV vector could increase both protective humoral and cellular responses. We engineered an ALVAC-SIV coexpressing CD40L with SIV_{mac251} (ALVAC-SIV/CD40L) *gag*, *pol*, and *env* genes. We compared its immunogenicity in macaques with that of a canonical ALVAC-SIV, with both given as a vector-prime/gp120 in alum boost strategy. The ALVAC-SIV/CD40L was superior to the ALVAC-SIV regimen in inducing binding and tier 1 neutralizing antibodies against the gp120. The increase in humoral responses was associated with the expression of the membrane-bound form of the CD40L by $CD4^+$ T cells in lymph nodes. Unexpectedly, the ALVAC-SIV/CD40L vector had a blunting effect on $CD4^+$ Th1 helper responses and instead favored the induction of myeloid-derived suppressor cells, the immune-suppressive interleukin-10 (IL-10) cytokine, and the down-modulatory tryptophan catabolism. Ultimately, this strategy failed to protect macaques from SIV acquisition. Taken together, these results underlie the importance of balanced vaccine-induced activating versus suppressive immune responses in affording protection from HIV.

IMPORTANCE CD40-CD40 ligand (CD40L) interaction is crucial for inducing effective cytotoxic and humoral responses against pathogens. Because of its immunomodulatory function, CD40L has been used to enhance immune responses to vaccines, including candidate vaccines for HIV. The only successful vaccine ever tested in humans utilized a strategy combining canarypox virus-based vector (ALVAC) together with an envelope protein (gp120) adjuvanted in alum. This strategy showed limited efficacy in preventing HIV-1/SIV acquisition in humans and macaques. In both species, protection was associated with vaccine-induced antibodies against the HIV en-

Citation Silva de Castro I, Gordon SN, Liu J, Bissa M, McKinnon K, Trinh HV, Doster MN, Schifanella L, Liyanage NP, Cao J, Cheng O, Foulds K, Roederer M, Koup RA, Shen X, Tomaras GD, Venzon DJ, Forthal DN, Fouts T, Montefiori DC, Tartaglia J, Rao M, Ostrowski M, Franchini G, Vaccari M. 2020. Expression of CD40L by the ALVAC-simian immunodeficiency virus vector abrogates T cell responses in macaques. J Virol 94:e01933-19. https://doi.org/10.1128/JVI.01933-19.

Editor Guido Silvestri, Emory University

Address correspondence to Genoveffa Franchini, franchig@mail.nih.gov, or Monica Vaccari, vaccarim@mail.nih.gov.

* Present address: Namal P. Liyanage, Department of Microbial Infection and Immunity, College of Medicine, Ohio State University, Columbus, Ohio, USA.

Received 15 November 2019
Accepted 5 December 2019
Accepted manuscript posted online 2 January 2020
Published 28 February 2020

velope and CD4$^+$ T cell responses, including type 1 antiviral responses. In this study, we tested whether augmenting CD40L expression by coexpressing it with the ALVAC vector could increase the protective immune responses. Although coexpression of CD40L did increase humoral responses, it blunted type 1 CD4$^+$ T cell responses against the SIV envelope protein and failed to protect macaques from viral infection.

KEYWORDS CD4, CD40L, HIV, MDSC, NHP, SIV, vaccine, macaques

In recent years, human immunodeficiency virus (HIV) incidence and mortality have declined globally due to a combination of prevention and treatment strategies, including antiretroviral treatment and public health education. However, a safe and effective prophylactic vaccine is urgently needed to ultimately control the human immunodeficiency virus type 1 (HIV-1) pandemic (1, 2). The only HIV-1 vaccine proven to be partially effective in a phase III clinical trial is a vaccination regimen based on an ALVAC expressing HIV-1 Env (gp120TM)/Gag/Pro as prime and bivalent HIV-1 rgp120/alum formulation booster administrations (3). The efficacy of this vaccine was 60% during the initial 12 months postvaccination but fell to 31.2% at the 42-month time point (3, 4). The waning of vaccine efficacy coincided with a rapid decline of HIV-1 Env V1/V2-specific IgG responses, in particular the IgG3 isotype, which was associated with a reduced risk of infection (4–8). In the setting of low anti-Env IgA, reduction in the risk of infection was seen in vaccinees that had high levels of antibody-dependent cell-mediated cytotoxicity (ADCC) and neutralization (9, 10). Multiplex bead array performed on a set of samples in an RV144 case-control study also revealed that the presence of a set of Th1, Th2, and T follicular helper (T_{FH}) cell-type cytokines was associated with a lower risk of HIV acquisition in humans (11, 12). Additional strategies building on the immunogenicity of the RV144 regimen may lead to better efficacy (4, 13).

We developed a macaque model that mimics the results of RV144 (14–16) and showed that an ALVAC-simian immunodeficiency virus (SIV)/gp120 alum strategy could protect macaques from intrarectal low dose challenges with a highly pathogenic, difficult to neutralize SIV_{mac251} strain. As in humans, protection of macaques against SIV_{mac251} acquisition was significant, but limited (vaccine efficacy, 44%), and did not impact postchallenge plasma virus levels in infected macaques (15). Similarly, in macaques, protection was mediated by antibodies and Th1 and Th2 CD4$^+$ T cells. Using the macaque model, we then tested strategies to increase the immunogenicity and effectiveness of the ALVAC/gp120 alum regimen by changing the adjuvant (15), the immunization used as prime (17), or the conformation of the gp120 protein to a full-length single chain (FLSC) (18). In parallel with these studies, we hypothesized that the costimulatory molecule, CD40 ligand (CD40L, CD154), may be used to modulate the priming capacity of the ALVAC vector and enhance the efficacy and durability of the ALVAC-HIV/rgp120 prime/boost regimen.

CD40L belongs to the tumor necrosis factor superfamily (TNFSF) (19, 20). In its membrane-bound form, CD40L is mainly expressed on activated CD4$^+$ T cells, while its receptor, CD40, is expressed on immature dendritic cells (DCs), B cells, and other immune and nonimmune cells. By engaging CD40 on immature dendritic cells, CD40L induces the maturation and activation of DCs, which in turn induce activation of cytotoxic CD8$^+$ T cells (cytotoxic T lymphocytes [CTLs]) (21). Ligation of CD40 on B cells by CD40L can promote B cell proliferation and survival, antibody isotype switching, and antibody affinity maturation (22, 23). CD40L plays a pivotal role in the development of both cellular and humoral memory immune responses and has been tested as an adjuvant to augment vaccine-induced immune responses including HIV-1/SIV vaccines (24–31). Recently, Kwa et al. reported that CD40L coexpressed with SIV antigens encoded by the viral vector modified vaccine Ankara (MVA) (DNA prime/MVA boost SIV vaccine) enhanced SIV-specific humoral and cellular immune responses, improved protection against SIV infection, and reinforced control of SIV replication in rhesus macaques (26, 27). We have previously shown in mice that CD40L expressed from an

ALVAC vector enhances memory polyfunctional CTL responses elicited by an ALVAC-HIV-1 vaccine (24).

To test whether CD40L increases the effectiveness of the ALVAC/gp120-alum regimen, we engineered an ALVAC-SIV vector that coexpresses rhesus macaque CD40L with SIV Env, Gag, and Pro proteins of $SIV_{mac251\text{-}K6W}$ (32), and we tested its immunogenicity and efficacy against repeated low-dose mucosal challenges of SIV_{mac251} in macaques (14, 15). We found that the coexpression of CD40L enhanced humoral immune responses elicited by the ALVAC-SIV prime-gp120 boost, including antibody responses against the V2-loop region of the gp120 protein, a correlate of decreased risk of HIV/SIV acquisition (5, 14, 15). Surprisingly, the coexpression of CD40L with the antigens within the ALVAC-SIV vaccine completely abrogated Env-specific Th1 $CD4^+$ T cell responses. It is possible that this decrease may be due to the concomitant increase we observed in the levels of myeloid-derived suppressor cells (a correlate of increased risk of SIV acquisition [33]), the suppressive cytokine interleukin-10 (IL-10), and the down modulatory tryptophan catabolism pathway. Ultimately, this regimen did not afford protection from SIV_{mac251} acquisition.

RESULTS

ALVAC-SIV/CD40L + gp120 vaccine increases CD40L expression on $CD4^+$ T cells. We engineered the ALVAC-SIV vaccine construct (vCP180) (32) to express SIV Env/Gag-pro together with rhesus macaque CD40L in its membrane-bound form (ALVAC-SIV/CD40L) (Fig. 1A and B). Surface staining with antibodies against the CD40L on HEK293T cells infected *in vitro* was positive only with this vaccine but not with the parental vector control ALVAC-SIV (Fig. 1C). We vaccinated eight rhesus macaques with 10^8 PFU of ALVAC-SIV/CD40L given intramuscularly four times, at weeks 0, 4, 12, and 24 (Fig. 1D). A second group of 27 macaques was vaccinated with 10^8 PFU of recombinant ALVAC (vCP2432) expressing SIV genes *gag-pro* and gp120TM, but not CD40L (ALVAC-SIV), given at the same time and by the same route as previously reported (15, 18). All 35 macaques were boosted twice with bivalent monomeric-gp120 proteins (200 μg each), gp120-gD SIV_{mac251}-M766 (34) and gp120-gD SIV_{mac251}-CG7V SIV_{E660} (35), adjuvanted in alum (Alhydrogel) and given at weeks 12 and 24 in the contralateral thigh of the vector immunization. Forty-seven macaques were used as controls as previously described (Fig. 1D) (15).

In its membrane-bound form, CD40L is transiently expressed on activated T cells (36). We tested whether the two vaccine strategies differently influenced the expression levels of CD40L on $CD4^+$ T cells. To this end, we stained cells isolated from peripheral lymph nodes (LNs) from 6 animals per group at week 13 (1 week after the third immunization) (Fig. 1D), as shown by representative density plots in Fig. 1E. Interestingly, ALVAC-SIV/CD40L-vaccinated animals had higher percentages of $CD40L^+$ $CD4^+$ T cells in LNs than those of animals vaccinated with ALVAC-SIV vaccine ($P = 0.041$, Mann-Whitney test) (Fig. 1F).

CD40L expression on $CD4^+$ T cells is associated with antibody titers to gp120 and neutralization. Serum was obtained from all animals in the study 1 week following the last immunization (week 25) (Fig. 2). We found that both vaccine regimens elicited high-titer binding antibodies against the bivalent gp120 proteins used in the boost vaccination, M766 from SIV_{mac251} and CG7V from SIV_{smE660} (Fig. 2A and B). Animals vaccinated with the CD40L-expressing vaccine displayed significantly higher binding antibody titers for both gp120 proteins compared to those of the ALVAC-SIV/gp120 strategy for SIV_{mac251} gp120 ($P < 0.001$) and for SIV_{smE660} gp120 ($P = 0.0002$, Cochran-Armitage test) (Fig. 2A and B). We found a direct association between the titers of antibodies to the SIV_{mac251} gp120 and the levels of $CD4^+$ T cells expressing the CD40L molecule when both groups of vaccinated animals were considered together (ALVAC-SIV + ALVAC-SIV/CD40L, $n = 12$; $R = 0.63$; $P = 0.033$; Spearman test) (Fig. 2C).

The expression of CD40L on $CD4^+$ T cells and their interaction with $CD40^+$ B cells regulate the development of germinal centers and affect the quantity and quality of antibody responses (22, 37). Indeed, a CD40L adjuvant for a DNA/MVA vaccine en-

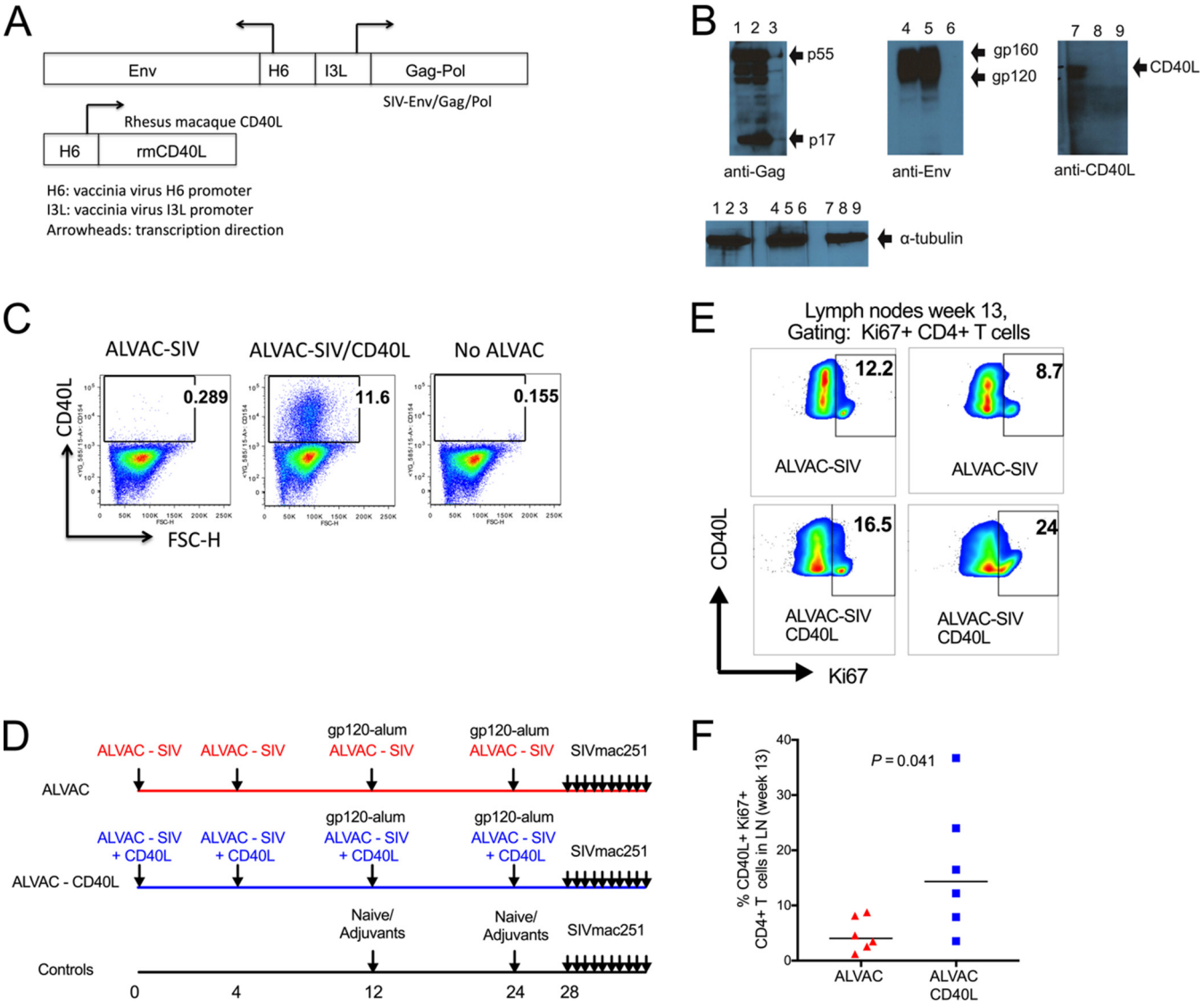

FIG 1 Vaccine and study design. (A) SIV gene cassette and CD40L gene cassette in ALVAC-SIV/CD40L. The SIV *env* and *gag/pol* genes were cloned into the C5 locus of ALVAC virus, and rhesus macaque *CD40L* gene was cloned into the C3 locus of the ALVAC virus. (B) ALVAC-SIV vaccine coexpression of rhesus macaque CD40L. (Lanes 1, 4, 7) ALVAC-SIV-CD40L. (Lanes 2, 5, 8) ALVAC-SIV. (Lanes 3, 6, 9) Mock infection. α-Tubulin was used as the loading control. (C) Expression of CD40L on the surface of HEK293T cells inoculated with 25 MOI of control ALVAC-SIV, ALVAC-SIV/CD40L, and medium. (D) Vaccination and challenge schedule. The arrows represent the time (weeks) of vaccination (0 to 24 weeks) or challenge (28 weeks). (E) Representative flow cytometry plots for 2 animals in both vaccine groups, showing the levels of CD40L expression on $CD4^+$ T cells from peripheral lymph nodes collected at 1 week after the first ALVAC/gp120-alum boost (week 13). Cells were gated on live $CD3^+$ $CD4^+$ $Ki67^+$ population. (F) Frequencies of $CD40L^+$ $CD4^+$ T cells in 6 macaques from each group are shown with the medians, represented by black lines.

hanced the functional quality of anti-Env antibody in macaques (27). We compared the functional quality of anti-Env antibodies in the two groups of ALVAC-SIV-vaccinated macaques. Both groups had high titers of neutralizing antibodies against the tier 1 $SIV_{mac251.6}$, but neutralization was higher in the CD40L group than in the ALVAC-SIV group ($P = 0.017$ by the Mann-Whitney test; week 25) (Fig. 2D). No animal serum samples were able to neutralize tier 2 SIV viruses or the SIV_{mac251} challenge stock virus (data not shown). We found a positive association between neutralization against $SIV_{mac251.6}$ and the levels of $CD4^+$ T cells expressing the CD40L molecule when both groups of vaccinated animals were considered together (ALVAC-SIV + ALVAC-SIV/CD40L, $n = 12$; $R = 0.60$; $P = 0.043$; Spearman test) (Fig. 2E). Moderately strong positive correlations within each vaccinated group were also found (data not shown), supporting a direct association between CD40L levels and neutralization. These data suggest

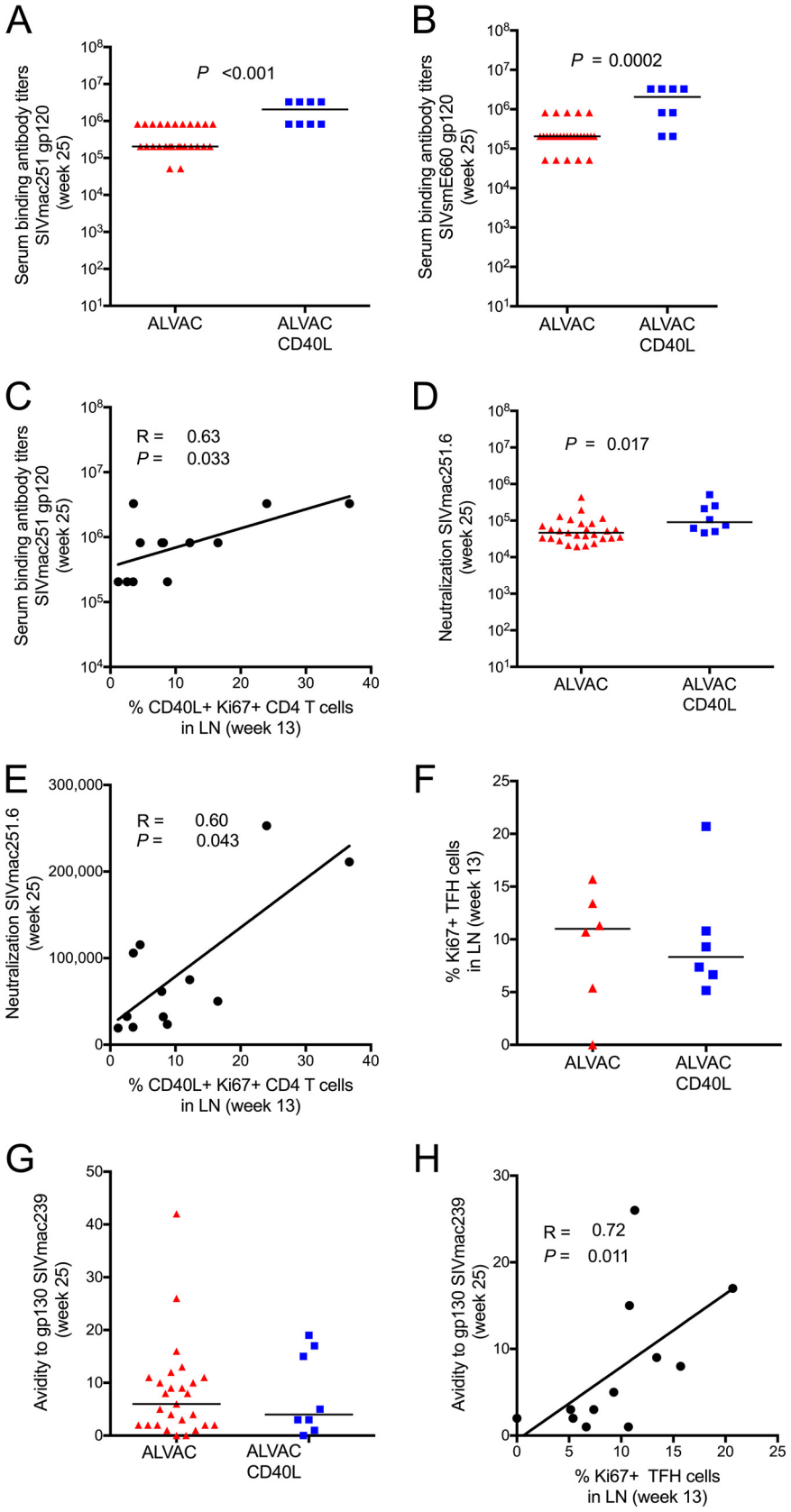

FIG 2 B cell responses are increased by CD40L expression. Titers of serum IgG binding to gp120 of SIV_{mac251}M766 (A) measured by ELISA (week 25) in the 2 vaccinated groups and of SIV_{smE660}CG7V (B). (C) Association with the frequency of $CD40L^+$ $Ki67^+$ $CD4^+$ T cells in lymph nodes (LNs) (ALVAC + CD40L

(Continued on next page)

that the expression of CD40L on vaccine-induced ($Ki67^+$) $CD4^+$ T cells affects both the quantity (titers) and the function (neutralization) of antibodies against SIV_{mac251} gp120.

A positive association between the breadth of neutralization and levels of T follicular helper (T_{FH}) cells in secondary lymphoid tissues has been previously described (38). We measured the frequency of T_{FH} cells in peripheral LNs collected at week 13 as $CD4^+$ T cells expressing high levels of CXCR5 and the programmed cell death protein 1, PD1 molecule ($CXCR5^+$ $PD1^{hi}$), by flow cytometry. The percentage of total T_{FH} cells did not differ between vaccines (Fig. 2F) at the time point analyzed. Accordingly, the avidity index measured in serum against SIV_{mac239} gp130 by enzyme-linked immunosorbent assay (ELISA) did not differ between the two vaccine groups (Fig. 2G). As expected from our previous studies (39), T_{FH} cell levels positively associated with the avidity index ($R = 0.72$ and $P = 0.011$ by the Spearman test) (Fig. 2H) in all vaccinated animals (40).

Increases in serum and rectal cV2 and V3 IgG do not translate to better protection against acquisition in the CD40L group. We measured the breadth of the gp120-binding antibody from vaccinated macaques using 89 overlapping linear peptides spanning the full length of the SIV_{mac251} gp120 protein by ELISA (Fig. 3). Both ALVAC prime-gp120 boost regimens elicited broad binding antibody responses against nearly every constant and variable region in gp120 (Fig. 3A). Plasma IgG responses to linear epitopes in the V2 and V3 regions of HIV-1 gp120 were correlated with a reduced risk of infection in the RV144 vaccine efficacy trial (10). Statistical analysis of the difference in antibody binding to each of the 89 peptides between the 2 groups indicated that the ALVAC-SIV/CD40L vaccine significantly increased antibody binding to 8 of the 89 peptides encompassing regions in V1, C2, and V3 (Fig. 3B).

Plasma IgG binding to scaffolded HIV-1 Env V1/V2 correlated with reduced risk of HIV-1 infection in the RV144 clinical trial (5). Similarly, IgG in rectal secretions binding to the cyclic V2 (cV2) peptide of SIV Env correlated with reduced risk of SIV infection in macaques receiving an ALVAC prime-gp120 boost vaccination (15, 18). We tested whether CD40L augments the V1/V2 binding antibodies and found that macaques vaccinated with ALVAC-SIV-CD40L had higher titers of serum IgG binding to scaffolded Env V1/V2 from $SIV_{mac239cs}$ ($P = 0.041$) (Fig. 3C). Serum IgG binding to scaffolded Env V1/V2 from another SIV strain, $SIV_{mac251WY}$, was also stronger in ALVAC-SIV/CD40L/gp120- than in ALVAC-SIV/gp120-immunized animals, though the difference did not reach a P of <0.05 level (data not shown). No difference was found in the titers of IgG against the V1/V2 of the SIV_{smE660} strain (Fig. 3D). Animals in the CD40L group had a higher titer of serum IgG binding to cyclic V2 (cV2) from both SIV_{mac251} and SIV_{smE543} than that of animals immunized with the ALVAC-SIV/gp120 vaccine ($P = 0.047$ and $P = 0.004$, respectively) (Fig. 3E and F). Interestingly, IgG binding to cV2 from both SIV_{mac251} and SIV_{smE543} in rectal secretions was also higher in ALVAC-SIV/CD40L-vaccinated animals at 2 weeks before the challenge (SIV_{mac251}, $P = 0.039$; SIV_{smE543}, $P = 0.018$; week 25, by the Mann-Whitney test) (Fig. 3G and H). Despite the increase in antibody responses against the gp120, and in particular against the V2 loop, the CD40L vaccine did not reduce the risk of SIV_{mac251} acquisition ($P = 0.747$ by the log rank test, Fig. 3I).

CD40L induces high levels of IL-4 and IL-21 after immunization with the gp120 alum protein. The increase in CD40L expression in LNs could suggest an increase in T follicular cells, providing helping signals to germinal center (GC) B cells. Thus, we measured the frequency of T_{FH} cells in lymph nodes. Interestingly, we could not detect a difference in the frequency of T_{FH} cells at 1 week after the 3rd immunization at this

FIG 2 Legend (Continued)
group, $n = 13$) at week 13 and IgG binding to gp120 of SIV_{mac251}M766. Serum neutralization 50% infective dose (ID_{50}) titers against tier 1 $SIV_{mac251.6}$ at week 25 (D) and correlation with the levels of $CD40L^+$ $Ki67^+$ $CD4^+$ T cells in LNs (ALVAC + CD40L group, $n = 13$) at week 13 (E). Percentage of $Ki67^+$ T_{FH} ($CXCR5^+$ $PD1^{hi}$) cells in peripheral LNs at week 13 ($n = 6$ each group) (F), avidity index in plasma at week 25 (G), and their correlations when all vaccinated animals are considered ($n = 12$, by the Spearman test) (H). In all dot plots, the median is shown.

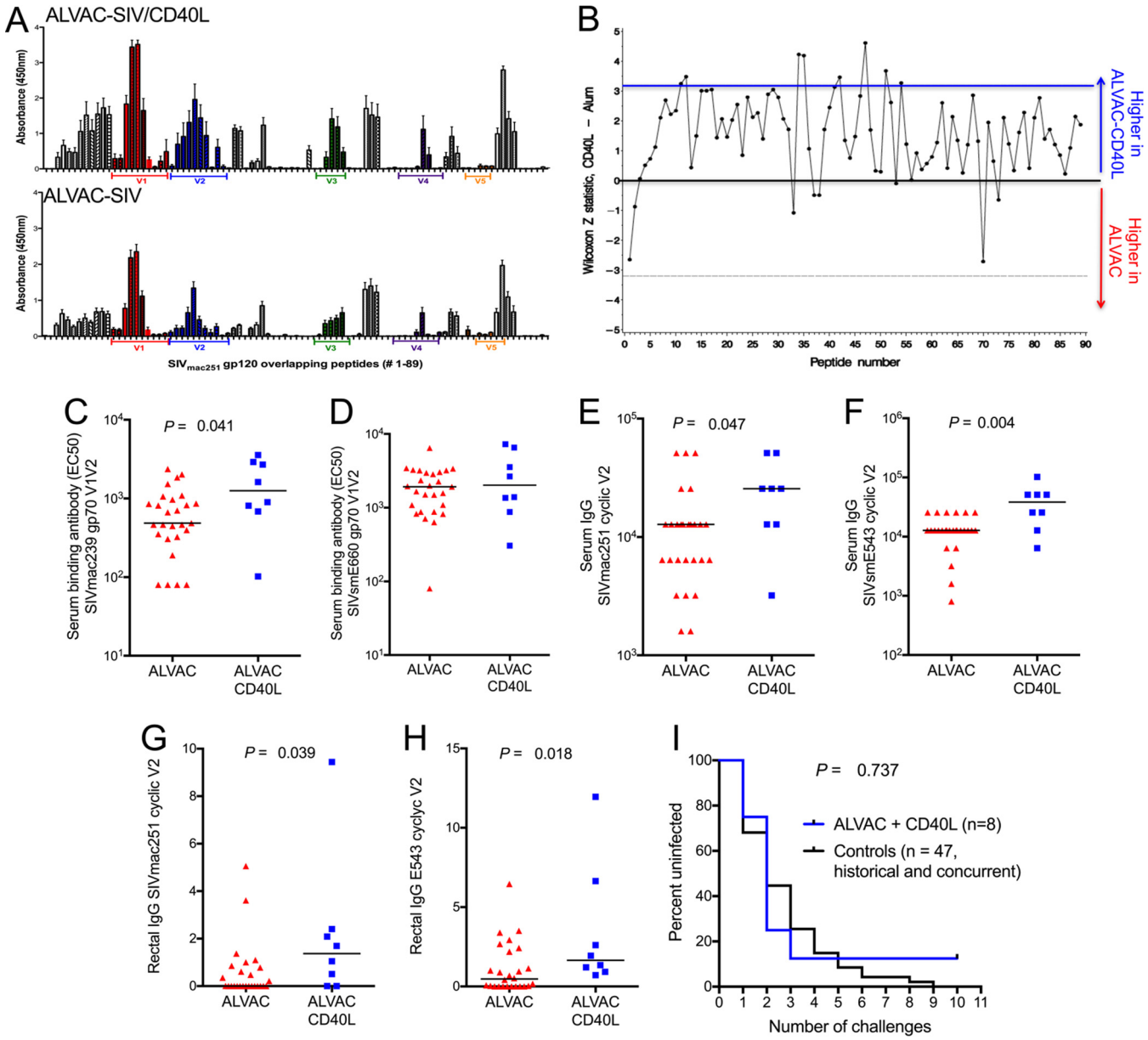

FIG 3 Increased breath of gp120 antibody responses does not translate to protection from acquisition. (A) Peptide binding measured as serum IgG binding to 89 overlapping linear peptides spanning SIV gp120 measured by ELISA for each single peptide for all of the animals in both vaccines. (B) Comparison of peptide binding measure for each single peptide. The Wilcoxon Z statistic was used. The blue and black dashed lines represent the statistically significant higher binding threshold for ALVAC-SIV/CD40L versus ALVAC-SIV and ALVAC-SIV versus ALVAC-SIV/CD40L, respectively, after correction for multiple comparisons by the Hochberg method. Serum IgG (EC50) binding to scaffolded SIV Env V1/V2 measured by BAMA against SIV_{mac239} (C) and SIVsmE660 (D). Titers of serum IgG binding to cyclic SIV Env V2 measured by ELISA against SIV_{mac251} (E) and SIV_{smE543} (F). Rectal cyclic SIV Env V2 (cV2)-specific IgG antibodies to SIV_{mac251} (G) and $SIV_{smE543-3}$ (H). (I) Percentage of uninfected animals in the ALVAC-SIV + CD40L prime-gp120 boost-vaccinated macaques (n = 8) versus control animals ($n = 47$). The log rank test was used.

site (Fig. 2F). We next compared the ability of the 2 recombinant ALVAC vectors to induce IL-4 and IL-21 cytokines providing help to B cells and found higher levels of IL-4 in the CD40L group than in the ALVAC group (Fig. 4A) ($P = 0.0003$ by the Mann-Whitney test) following *in vitro* stimulation of peripheral blood mononuclear cell (PBMCs) with overlapping linear peptides that encompassed the SIV_{mac251} gp120 protein.

The levels of IL-4 were strongly positively associated with the titers of gp120 antibodies to SIV_{mac251} and SIV_{smE660} and with the levels of SIV_{smE543} cV2 in the serum at week 25 ($R = 0.59$, $P = 0.052$; $R = 0.67$, $P = 0.033$; $R = 0.62$, $P = 0.020$, respectively,

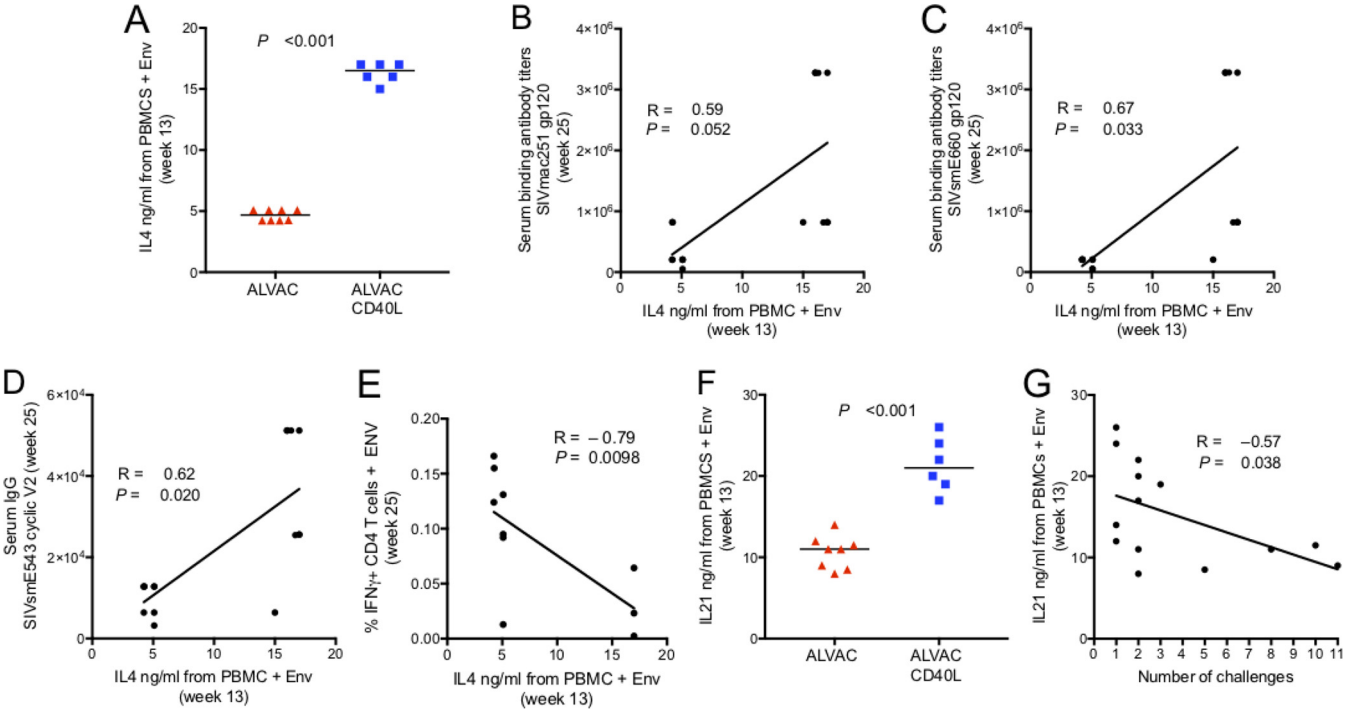

FIG 4 IL-4 and IL-21 are increased by the ALVAC coexpressing the CD40L. (A) Levels of IL-4 released by PBMCs at week 13 (ALVAC, $n = 8$; CD40L, $n = 6$), following stimulation with overlapping gp120 peptides. The Mann-Whitney test was used to determine P values, and the median is shown. Correlations between the IL-4 levels and the titers of antibodies measured in plasma (B to D) and with the percentage of env-specific IFN-g$^+$ CD4$^+$ T cells in blood at week 25 in all the vaccinated animals (ALVAC-SIV and ALVAC-SIV/CD40L) (E). The Spearman test was used. (F) Levels of IL-21 cytokine produced by PBMCs after stimulation with overlapping gp120 peptides (week 13). (G) Association between the IL-21 and the number of challenges to infection.

by the Spearman correlation and the Jonckheere-Terpstra test) (Fig. 4B to D). No associations were found when the two vaccinated groups were analyzed separately. Moreover, the levels of IL-4 were inversely correlated with the percentage of CD4$^+$ T cells producing gamma interferon (IFN-γ) and tumor necrosis factor alpha (TNF-α) ($R = -0.79$, $P = 0.008$; $R = -0.78$, $P = 0.019$ by the Spearman test) (Fig. 4E and data not shown) when all groups were pooled together.

Similar to what we observed for IL-4, the level of IL-21 measured by Luminex in total PBMCs was also significantly higher in the CD40L group than in the ALVAC-SIV/gp120 group (Fig. 4F). No association was found between IL-21 levels and CD4$^+$ T cell responses or with antibody responses or the frequency of T_{FH} cells (data not shown). Interestingly, IL-21 levels were associated with increased risk of SIV acquisition ($R = -0.59$; $P = 0.038$ by the Spearman test) (Fig. 4G).

CD40L abrogates the generation of envelope-specific Th1 responses. We and others have previously reported associations of vaccine-induced T helper CD4$^+$ T cells with the risk of SIV or HIV acquisition in macaques (10, 12) and humans (12). We assessed Env-specific T cell responses using flow cytometry. PBMCs from macaques were stimulated with a peptide pool encompassing the whole region of the SIV_{mac251} gp120, and production of IFN-γ, TNF-α, and IL-2 by CD4$^+$ and CD8$^+$ T cells was measured by flow cytometry. Compared to ALVAC-SIV-immunized macaques, CD4$^+$ T cells from ALVAC-SIV/CD40L-vaccinated animals produced lower amounts of IFN-γ and IL-2 cytokines in the blood at week 5 after two ALVAC-SIV vaccinations ($P = 0.032$ and $P = 0.003$ by the Fisher exact test, respectively) (Fig. 5). Only three of seven animals were positive for TNF-α in the ALVAC group, as none were in the ALVAC-SIV/CD40L group ($P = 0.19$) (Fig. 5A to C). Strikingly, IFN-γ, TNF-α, and IL-2 cytokines remained substantially lower in the ALVAC/CD40L group at the end of the vaccination regimen at week 25 ($P = 0.011$, $P = 0.023$, and $P = 0.037$ by the Mann Whitney test, respectively) (Fig. 5D to F). CD4$^+$ T cells from ALVAC-SIV/CD40L-vaccinated macaques also showed

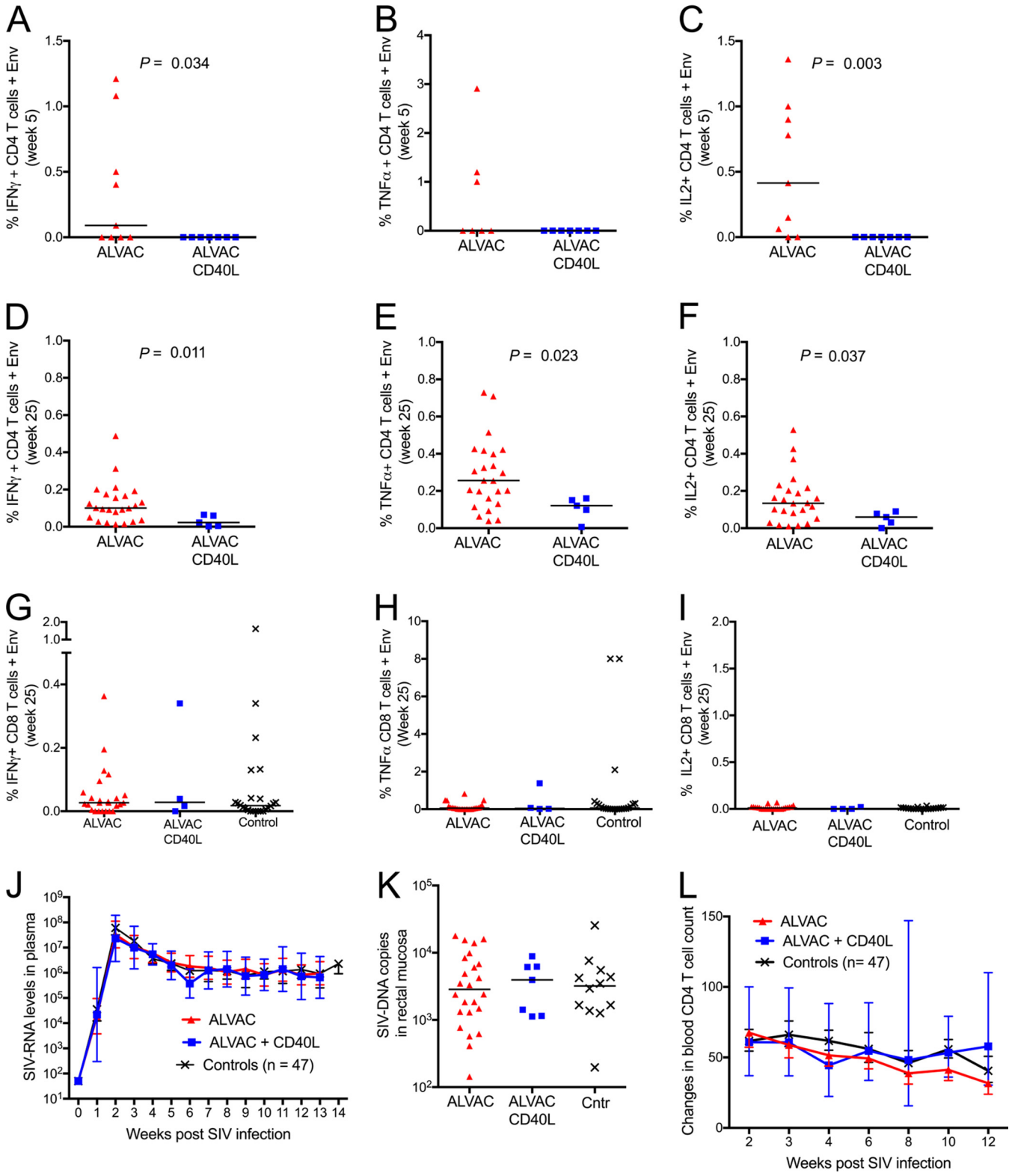

FIG 5 ALVAC-SIV/CD40L vaccine decreases Env-specific Th1 responses. Percentage of envelope-specific $CD4^+$ T cells producing IFN-γ, TNF-α, and IL-2 in blood at week 5 (A to C), and at week 25 (D to F), following stimulation with overlapping gp120 peptides. (G to I) Percentage of envelope-specific $CD8^+$ T cells producing IFN-γ, TNF-α, and IL-2 at week 25. Fisher's exact test for positivity of values was used to determine *P* values, and the median is shown. (J) SIV RNA copies per milliliters plasma. The geometrical mean and standard error for both vaccines and controls (in black) is shown. (K) SIV-DNA levels in rectal mucosa at 3 weeks after infection. (L) Mean ± standard deviation of the number of $CD4^+$ T cells in blood after infection with respect to the preinfection count. The standard deviation is shown.

fewer polyfunctional responses to the SIV_{mac251} gp120, although the difference was within the range of standard variation (data not shown). As previously described for the ALVAC-SIV/gp120 alum strategy (3, 18), little or no cytokine production was detected in $CD8^+$ T cells after envelope peptide stimulation in all macaques at the end of the immunization (week 25) regardless of the vaccination received (Fig. 5G to I). Accordingly, protection from high viral replication was not observed in the vaccinated macaques that became infected, as plasma viral load (Fig. 5J), DNA-SIV level in the rectal mucosa (Fig. 5K), or $CD4^+$ T cell count (Fig. 5L) did not differ between the vaccinated and control groups.

ALVAC-SIV/CD40L vaccination induces immune suppressive responses. We recently reported that myeloid cell cross talk regulates the efficacy of ALVAC- SIV-based vaccines and that the induction of myeloid-derived suppressor cells (MDSCs) plays a negative role in protection (33). Given the unexpected reduction in Th1 type responses against the SIV envelope by the ALVAC/CD40L vaccine, we hypothesized that this vaccination regimen may induce MDSCs. We analyzed the frequency of the MDSC-enriched population, that in macaques is defined as HLA-DR^- $CD14^+$ cells, by fluorescence-activated cell sorter (FACS) analysis (Fig. 6) (33, 41). When compared to the ALVAC-SIV group, the ALVAC-SIV/CD40L group presented significantly higher levels of HLA-DR^- $CD14^+$ cells in the blood at week 13 ($P = 0.024$ by the Mann Whitney test) (Fig. 6A). MDSC suppressive function includes the secretion of immune suppressive cytokines, such as IL-10, and the induction of the tryptophan pathways (42). The accumulation of tryptophan metabolites blocks $CD4^+$ T cell proliferation (43). Following the gp120 and alum boost in both vaccines (week 13), the same shift toward immunosuppression by the ALVAC-SIV/CD40L vaccine was observed by analyzing the levels of PBMCs producing the immune suppressive IL-10 cytokine by Luminex ($P < 0.001$, Mann Whitney test) (Fig. 6B). The level of IL-10 was positively associated with the percentage of HLA-DR^- $CD14^+$ cells ($R = 0.68$ and $P = 0.025$ by Pearson, and $R = 0.58$ and $P = 0.085$ by Spearman test) (Fig. 6C). Interestingly, higher levels of kynurenine, a metabolite of the amino acid tryptophan, as well as a higher kynurenine to tryptophan ratio were also detected in the plasma of the CD40L group ($P = 0.057$ by the Mann Whitney test) (data not shown and Fig. 6D). The kynurenine/tryptophan ratio measured in plasma at week 5 was positively correlated with the IL-10 levels (week 13, $R = 0.85$, $P < 0.001$, Spearman test) (Fig. 6E) and negatively associated with the frequency of the T cell proliferation-inducing IL-2^+ $CD4^+$ T cells (week 5, $R = -0.70$, $P = 0.009$, Spearman test) (Fig. 6F).

Others have shown that the soluble form of CD40L induces/signals trough MDSCs (44) and mediates tryptophan (try) catabolism (45). Activated T-lymphocytes and platelets can release soluble CD40L (sCD40L) into circulation (46), which possesses immunosuppressive effects (44). We measured the levels of soluble CD40 ligand (sCD40L) in plasma. Levels of sCD40L were elevated in the serum of animals following two immunizations with the ALVAC-SIV/CD40L vector compared to those of the ALVAC-SIV vector (Fig. 6G) ($P = 0.075$ by the Mann-Whitney test). Indeed, in the ALVAC/CD40L-vaccinated animals, macaques that had higher sCD40L had lower levels of tryptophan ($R = -0.78$, $P = 0.030$, Spearman test) (Fig. 6H). Taken together, these results suggest that sCD40L may result in the suppression of Th1 cell responses by inducing immune suppressive responses (Fig. 7).

DISCUSSION

Cognate antigen binding to a B-cell receptor alongside CD40 ligand (CD40L or CD154) engagement with CD40 receptors leads to the generation of a successful adaptive immune response (47). Because of its role in this process, CD40L has been tested as an adjuvant for viral vaccines against influenza, herpes simplex virus (HSV), and HIV, and cancer (19, 26, 48). CD40L has also been tested as an HIV vaccine adjuvant in a DNA prime recombinant modified vaccine Ankara (MVA) boost strategy in rhesus macaques. Immunization with an SIV recombinant DNA expressing CD40L followed by an MVA-SIV boost significantly reduced the risk of viral acquisition after mucosal

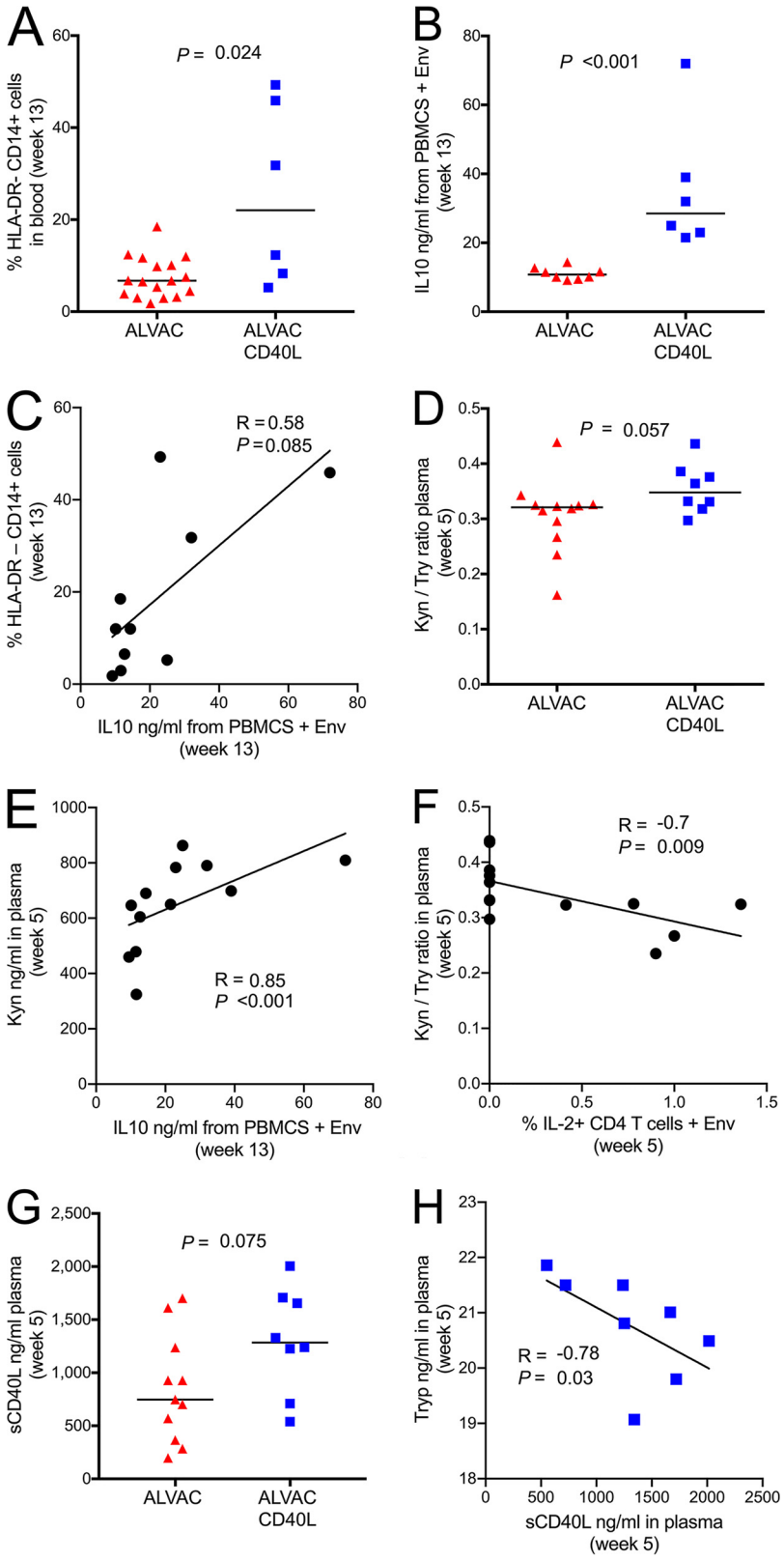

FIG 6 ALVAC-SIV/CD40L vaccine increases down modulatory cells and pathways. (A) Frequency of HLA-DR$^-$ CD14$^+$ cells in blood at week 13 (ALVAC, $n = 17$; CD40L, $n = 6$). Levels of IL-10 from PBMCs at week 13 stimulated with env peptides *in vitro* (ALVAC, $n = 8$; CD40L, $n = 6$) (B) and their association with the percentage of HLA-DR$^-$ CD14$^+$ cells (all vaccinated animals, $n = 10$) (C). (D) Ratio of kynurenine on tryptophan levels in plasma at week 5 measured by ELISA (ng/ml) (ALVAC, $n = 11$; CD40L, $n = 8$).

(Continued on next page)

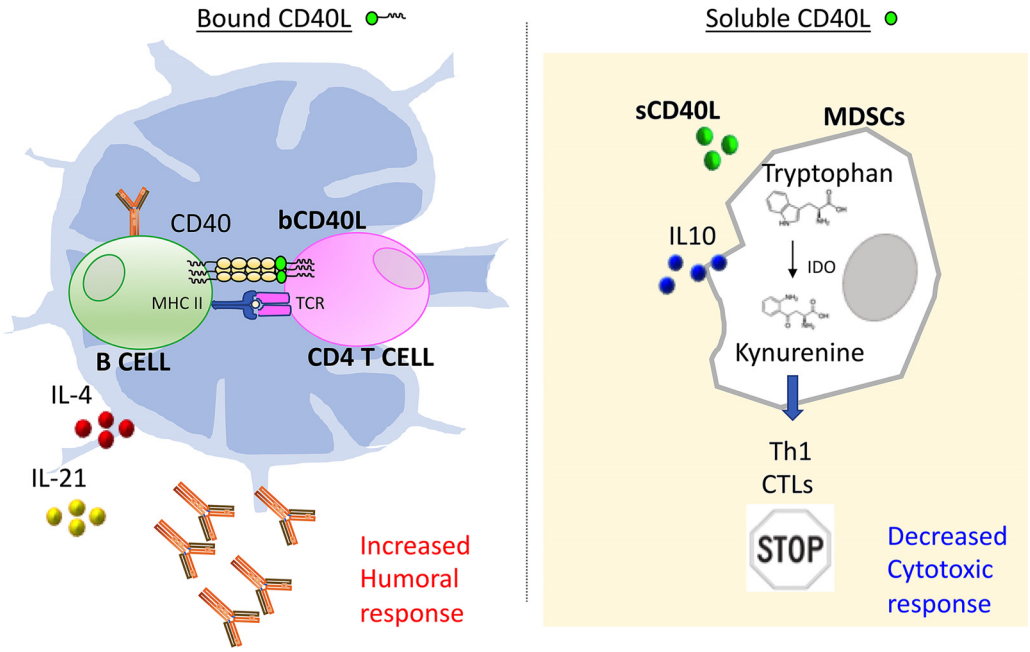

FIG 7 Results schematic.

exposure to the easy-to-neutralize SIV_{smE660} strain, with avidity and the neutralization index as correlates of protection (26). A similar vaccine, in which CD40L was expressed by both recombinant DNA and MVA, protected macaques from the difficult-to-neutralize, highly pathogenic SIV_{mac251} strain (27).

We tested the hypothesis that an ALVAC vector coexpressing SIV- Env/Gag-pro together with CD40L could improve SIV-specific humoral and cytotoxic responses, increasing the efficacy of the ALVAC-HIV/gp120 alum vaccine strategy. CD40L coexpression by the ALVAC-based vaccine resulted in increased levels of both the soluble and the bound form of CD40L, with the latter expressed by early activated $CD4^+$ T cells in lymph nodes. In the secondary lymphoid tissues, CD40L interaction with $CD40^+$ B cells induces T cell-dependent B cell proliferation, immunoglobulin production, and somatic hyper mutation (SHM) of the Ig to enhance affinity for antigens (49). Indeed, the coexpression of CD40L by the ALVAC-SIV/gp120 vaccine enhanced the titers of SIV Env-specific humoral immune response to both envelope proteins in our vaccine (SIV_{mac251} and SIV_{smE660}).

Consistent with the findings of Kwa et al. (26), we also observed increased neutralization to the tier 1 virus in the CD40L group that positively associated with the levels of $CD40L^+$ $CD4^+$ T cells in lymph nodes. Interestingly, there was no increase in antibody avidity by the expression of CD40L nor could we detect changes in T follicular helper cells at the single time point when we collected the LNs (week 13). At the same time, we observed an increase in IL-4 and IL-21 cytokine production by PBMCs after SIV-envelope *in vitro* stimulation. It is possible that the timing and/or the location of LN collection (away from the site of vaccination) may have impaired our ability to detect vaccine-induced changes in the T_{FH} cell level. Alternatively, the enhanced strength of the CD40L/CD40 signal alone may have increased antigen-responding B cells (37) without increasing T-mediated B cell help. It has been shown that the priming of the

FIG 6 Legend (Continued)
Association between the kynurenine (Kyn) tryptophan (Try) ratio in plasma and the levels of IL-10 ($n = 12$) (E) and with the frequency of IL-2^+ $CD4^+$ T cells ($n = 12$) (F). (G) Plasma levels of soluble CD40L at week 5 (ALVAC, $n = 11$; CD40L, $n = 8$). (H) Association between the plasma tryptophan levels and the sCD40L plasma levels in all the macaques in the ALVAC/CD40L group (week 5, $n = 8$). The Spearman test was used.

T cell compartment with an enhanced CD40 signal *in vivo* can result in transient enhancement of antigen-specific Ig levels, followed by premature termination of long-lived humoral immunity and B cell memory (37). In this scenario, nonhelped "low quality" B cells may be the source for the IL-4 and IL-21 cytokines rather than $CD4^+$ T cells.

Notably, the CD40L group had significantly higher titers of V1/V2 binding antibodies in serum and higher responses to IgG binding to SIV Env (cV2-IgG) cyclic V2 in serum and rectal secretions, which was previously found to be a correlate of decreased risk of acquisition in humans and macaques vaccinated with the ALVAC-SIV/gp120 alum strategy (5, 15, 18). Despite inducing a higher antibody response against the V2-loop, the CD40L vaccine did not protect macaques from SIV acquisition. Although we have previously described the cV2 responses as associated with protection, we also found that the quality of such responses may be important as well (15). In fact, our published results suggest that the different effects of cV2-IgG on risk of infection may depend on differences in glycosylation or isotype (7, 15, 50). Whether the expression of CD40L in the ALVAC also changed the glycosylation pattern or the isotype, and thus the effector functions of the elicited mucosal Env-specific antibodies, remains unknown. The difficulty of collecting enough mucosal secretion to perform this test prevented further investigation.

The ALVAC prime-gp120 boost elicited moderate $CD4^+$ T cell responses and negligible $CD8^+$ T cell responses against HIV-1/SIV in humans and rhesus macaques (3, 11, 14, 18). Th1 type responses have been described as correlates of protection both in humans and macaques vaccinated with ALVAC-based strategies (3, 15). CD40/CD40L binding activates dendritic cells and enhances cytotoxic $CD8^+$ T cell responses (21, 51, 52). Hence, a CD40L-adjuvanted DNA-MVA strategy resulted in increased T cell responses, particularly those of Th1 and cytotoxic $CD8^+$ T cells. Surprisingly, the addition of CD40L to the ALVAC vector did not enhance Th1 or $CD8^+$ T cell responses to the SIV envelope. Rather, it dramatically decreased envelope-specific Th1 $CD4^+$ T cell responses. It is possible that the different cytokine milieus induced by ALVAC and MVA may have played a role in decreasing the IFN-γ responses (53). In addition, the two vaccines may have induced different levels of CD40L signaling (54). Instead of inducing Th1-like responses, the CD40L group had increased levels of the suppressive IL-10 cytokine. This is not completely unexpected in that the CD40-CD40L costimulatory pathway plays a crucial role in the production of cytokines by monocytes and macrophages, including interleukin IL-10. Depending on the intensity of CD40L signaling, ligation of CD40 can promote either proliferation or apoptosis of $CD4^+$ T cells (44, 55). Interestingly, the heightened levels of IL-10 were associated with higher levels of suppressive myeloid cells (MDSCs) and increased tryptophan catabolism. We believe that these cells may have been induced by a strong signal from the soluble monomeric form of the CD40L molecule. In fact, this form of CD40L can be shed by activated T lymphocytes and possesses immunosuppressive effects (44). Here, we found an association between MDSCs and IL-10 cytokine levels. MDSCs produce IL-10 and induce the generation of T regulatory cells (42). Both these negative regulators can further suppress $CD4^+$ T cell proliferation by increasing the tryptophan catabolism.

The ALVAC-SIV/rgp prime/boost regimen that incorporated the coexpression of the costimulatory molecule CD40L in the ALVAC-SIV priming component failed to protect macaques from acquisition of the highly pathogenic SIV_{mac251}. Furthermore, IL-21 levels were correlated with the risk of infection, supporting the idea of the generation of a low-quality/brief B cell response. Moreover, the loss of Th1 responses may have contributed to the lack of protection by this strategy.

In conclusion, we found that CD40L enhanced humoral immune responses elicited by an ALVAC prime-gp120 boost SIV vaccine while simultaneously decreasing Th1-type responses to the envelope (IL-2, TNF-α, and IFN-γ) and increasing IL-10-producing MDSCs, as summarized in Fig. 7. These changes had a negative effect on protection from SIV acquisition in our macaque model. These results, coupled to prior data obtained by our group (15, 17) and by others (7, 12, 50), underline the importance of

more qualitative aspects of immune parameters and their interplay in affording protection in nonhuman primates (NHPs) and humans. As such, we need to gain a deeper appreciation of the importance of such composite biomarkers through an interplay between preclinical and clinical studies that also serve to validate their relevance to clinical outcomes.

MATERIALS AND METHODS

Vaccines. The ALVAC-SIV vaccine, vCP2432, is a canarypox vector that can express *gag-pro* and *gp120 TM* genes derived from a mucosal transmitted founder SIV_{mac251} M766 virus (56) as previously described (18). The ALVAC-SIV variant that coexpresses rhesus macaque CD40L, ALVAC-SIV/CD40L, was made as previously reported (57–59) (Fig. 1A). Briefly, cDNA encoding rhesus macaque CD40L under the control of a vaccinia virus early/late promoter H6 (60) was put into the C3 locus of vCP180, an ALVAC vector that can express *gag-pol* and *env* precursor (gp160) genes from $SIV_{mac251(K6W)}$ (32) by homologous recombination in chicken embryo fibroblasts (Charles River Laboratories, North Franklin, CT). The recombinant virus then underwent 6 consecutive rounds of plaque purification. Incorporation of the CD40L gene into the C3 locus was verified by plaque membrane hybridization with digoxigenin (DIG)-labeled rhesus macaque CD40L and C3 probes and PCR of purified virus DNA. The CD40L and C3 probes were made using a PCR DIG probe synthesis kit (Roche Diagnostics GmbH, Mannheim, Germany) according to the manufacturer's protocol. The sequences of the PCR primers for rhesus macaque CD40L are as follows: forward, 5′-GAAAGGAATCTTCATGAAGATTTTGT-3′; reverse, 5′-GGATTGTTGCCCGCAAGG-3′. The sequences of the PCR primers for C3 locus of vCP180 are as follows: forward, 5′-AACGTGCAGCAGACATA AACA-3′; reverse, 5′-ATAACAGCAGCTGTTCTACCAGTAGT-3′. Expression of CD40L and SIV Gag and Env proteins from ALVAC-SIV/CD40L was verified by Western Blotting analysis of cell lysates from HeLa cells infected with ALVAC-SIV/CD40L or its control ALVAC-SIV (vCP180) at 5 multiplicity of infection (MOI) for 2 days. Cell lysate was prepared using CelLytic M cell lysis reagent (Sigma-Aldrich, Oakville, ON, Canada) according to the manufacturer's protocol. Cell lysate was then subjected to SDS-PAGE using NuPage 4 to 12% bis-Tris gel (Invitrogen, Burlington, ON, Canada), transferred to a Hybond-P polyvinylidene difluoride (PVDF) membrane (GE Healthcare Life Sciences, Mississauga, ON, Canada) and probed with mouse anti-SIV_{mac251} p17 MAb (61), mouse anti-SIVmac251 gp120 MAb (61, 62) (both from NIH AIDS Reagent Program, Germantown, MD), and goat anti-human CD40L antibody (R&D Systems Inc., Minneapolis, MN), and detected with horseradish peroxidase (HRP)-labeled donkey-anti-mouse antibody or donkey-anti-goat antibody (both from Jackson ImmunoResearch Laboratories, West Grove, PA), respectively. The bivalent SIV gp120 proteins used were gp120-gD.M766 (gp120 from a mucosal transmitted SIV_{mac251} founder variant) (56) and gp120-gD.CG7V (gp120 from a mucosal transmitted SIV_{smE660} variant) (34). Both proteins have the herpes simplex virus glycoprotein D peptide tag at the N termini as did the gp120 proteins used in the RV144 trial. Both proteins were expressed in CHO cells and formulated with alum.

***In vitro* infection.** HEK293T cells were cultured in a 6-well plate overnight and inoculated with 25 MOI ALVAC-SIV/CD40L, control ALVAC-SIV, or just medium (no ALVAC control). Twenty-four hours later, cells were collected and stained with LIVE/DEAD fixable violet and phycoerythrin (PE)-labeled mouse anti-human CD40L (number 310805; BioLegend). Stained cells were run on LSRFortessa (BD Biosciences), and flow data were analyzed with FlowJo software (FlowJo LLC). Data shown were gated on single and live cells.

Animals, immunization, and SIV challenges. All animals were housed and handled according to the guidelines of the Association for the Assessment and Accreditation of Laboratory Animal Care International. This study was approved by the Institutional Animal Care and Use Committee at Advanced BioSciences Laboratories (Rockville, MD). A total of 82 rhesus macaques (*Macaca mulatta*) were used in this study and divided into 3 groups. Group 1 consisted of 27 macaques that were vaccinated in the quadriceps with 10^8 PFU ALVAC-SIV (vCP2432) at weeks 0, 4, 12, and 24 as described elsewhere (15). Group 2 had 8 animals that were vaccinated in the quadriceps with 10^8 PFU ALVAC-SIV/CD40L (vCP180 + CD40L) at weeks 0, 4, 12, and 24. Macaques in groups 1 and 2 were boosted with bivalent SIV gp120 proteins (200 μg for each protein) formulated in alum (Alhydrogel, 500 μl) at weeks 12 and 24 in the quadriceps opposite of the ALVAC-SIV vaccination site (15). Group 3 contained 24 simultaneous controls that received alum (6 animals) or MF59 (Novartis, 12 animals) at weeks 12 and 2 or were left untreated (6 animals). In addition, 23 historical controls were used that either received alum (11 animals) (14) or gp96-Ig (63). The study was not powered to compare efficacy between the 2 vaccination strategies. Four weeks after the final vaccination, all animals were challenged intrarectally each week with 120 $TCID_{50}$ (50% tissue culture infective dose) SIV_{mac251}. Animals testing negative for SIV RNA in plasma were rechallenged up to a maximum of 10 challenges.

SIV gp120 proteins and peptides binding antibody. Linear peptide mapping of serum was performed by ELISA. Sera collected at 1 week after the last immunization were diluted to 1:20 and added to plates coated with peptides encompassing the entire SIV_{K6W} gp120 amino acid sequence (34). The SIV Env-specific IgG and IgA antibodies in serum were determined by custom SIV bAb multiplex assay (SIV-BAMA) (64). Antibodies against native V1/V2 epitopes were quantitated by binding assays against SIV V1/V2 scaffold antigens expressed as gp70-fusion proteins related to the CaseA2 antigen used in the RV144 correlate study (provided by A. Pinter). These proteins contained the glycosylated, disulfide-bonded V1/V2 regions of SIV_{mac239}, SIV_{mac251}, and SIV_{smE660} (corresponding to amino acids [AA] 120 to 204 of HXB2 Env) fused to residue 263 of the SU (gp70) protein of Fr-MuLV.

SIV cyclic V2 binding antibody. SIV V2 peptide was synthesized by JPT Peptide Technologies GmbH (Berlin, Germany) as described elsewhere (18). The amino acid sequence of the SIV V2 peptide is based on the $SIV_{smE543-3}$ V2 domain from GenBank accession number U72748. The SIV V2 peptide sequence contains an N-terminal biotin tag with sequences as follows: GF SIVsmE543 CIKNNSCAGLEQEPMIGCKF NMTGLKRDKKIEYNETWYSRDLICEQPANGSESKCY; GF SIVmac251 full length sequence CIAQNNCTGLEQEQ MISCKFNMTGLKRDKTKEYNETWYSTDLVCEQGNSTDNESRCY CM5 chips and the Biacore amine coupling kit were purchased from GE Healthcare (Piscataway, NJ). Streptavidin was purchased from Invitrogen (Grand Island, NY). Affinity purified goat anti-monkey IgG and IgA (gamma chain- or alpha chain-specific) antibodies were purchased from Rockland Immunochemicals (Gilbertsville, PA).

Surface plasmon resonance (SPR) measurements were conducted with a Biacore T200 using the CM5 chip as described previously (15). Streptavidin was immobilized onto the chip using the amine coupling kit as directed by the immobilization wizard packaged with the T200 control software. A total of 6,700 response units (RU) of 1 μM streptavidin in 20 mM sodium formate, pH 4.2 (10-min contact time, 10-μl/min flow rate) was immobilized. The biotinylated peptide was prepared at a concentration of 1 μM in 20 mM Tris, pH 7.4, and allowed to flow (at 10 μl/min) over the streptavidin-coated surface of flow cell 4 until 3,500 RU of SIV V2 peptide was captured.

The mucosal swabs were thawed on ice and centrifuged at 16,100 relative centrifugal force (rcf), 4°C, for 5 min. The supernatant was diluted 10-fold in Tris-buffered saline (TBS), pH 7.4, and then analyzed on the Biacore. The diluted mucosal samples were passed over the chip surface at a flow rate of 30 μl/min for 3 min followed by a 5-min dissociation period. At the end of the 5-min period, a 20 μg/ml solution of affinity-purified gamma chain-specific goat anti-monkey IgG or IgA antibody was passed over the peptide coated Ig-bound surface for 2 min at a flow rate of 10 μl/min. After a 70-s dissociation period, the chip surface was regenerated, and data were analyzed using the BIAevaluation 4.1 software. The reported response units (RU) for the IgG- or IgA-specific values are the difference between the average value of a 5-s window taken 60 s after the end of the anti-IgG or anti-IgA injection and the average value of a 5-s window taken 10 s before the beginning of the anti-IgG or anti-IgA injection. The data (RU) are presented as dot plots for individual mucosal samples.

For determining the total IgG antibodies in the mucosal samples, anti-IgG immobilization on a CM5 chip was performed using 100 nM unconjugated gamma chain-specific goat anti-monkey IgG (Rockland Inc., Gilbertsville, PA) in 20 mM sodium acetate, pH 4.2, with a 5-min contact time and a 10-μl/min flow rate resulting in the immobilization of 9,100 RU. Centrifuged mucosal samples (diluted 1:10) were passed over the chip surface at a flow rate of 30 μl/min for 3 min, followed by a 5-min dissociation period. The relative amount of monkey IgG was determined using the same secondary injection and analysis strategy described above.

Chemstrips were used to determine the blood contamination in mucosal samples. Ten microliters of the mucosal supernatant sample was spotted onto a Chemstrip 5 OB urine test strip (ref number 11893467-160; Roche). After 60 s, any change in color was recorded for comparison to the manufacturer's color chart.

Neutralizing antibody. Neutralization was measured as a reduction in luciferase reporter gene expression after a single round of infection in TZM-bl cells as described previously (65, 66). TZM-bl cells were obtained from the NIH AIDS Research and Reference Reagent program, as contributed by John Kappes and Xiaoyun Wu. Two hundred $TCID_{50}$ of virus was incubated with serial 3-fold dilutions of test sample in duplicate in a total volume of 150 μl for 1 h out of 18 h at 37°C as indicated in 96-well flat-bottom culture plates. Freshly trypsinized cells (10,000 cells in 100 μl of growth medium containing 75 μg/ml DEAE-dextran) were added to each well. One set of control wells received cells and virus (virus control), and another set received cells only (background control). After 48 h, 100 μl of cells was transferred to 96-well black solid plates (Costar) for measurements of luminescence using the Britelite luminescence reporter gene assay system (PerkinElmer Life Sciences). Neutralization titers are the dilution at which relative luminescence units (RLU) were reduced by 50% compared to that in virus control wells after subtraction of background RLUs.

Assay stocks of molecularly cloned Env-pseudotyped viruses (SIV_{mac251} CS.41, SIV_{mac239} 0.23, SIV_{mac251} WY:30) were prepared by transfection in 293T cells and were titrated in TZM-bl cells as previously described (67). Assay stocks of uncloned T-cell line-adapted (TCLA) SIV_{mac251} and SIV_{mac251} CS/2002 Letvin were produced in H9 and human PBMCs, respectively, and were titrated in TZM-bl cells.

Avidity index capture ELISAs. High-binding plates were coated with 1 mg/ml of a sheep polyclonal antibody specific to Env LAV1 (D7324 Ab; Aalto Bio Reagents) overnight at 4°C. The plates were washed 3× with 400 μl/well with 1× Tris-buffered saline with Tween 20 (TBST) in an automated plate washer, blocked with Blotto buffer (5%, wt/vol, nonfat milk in 1× TBST) for 1 h, and washed again as before. SIVmac239 gp130 was added to the plates at 1 μg/ml, incubated for 1 h, and washed again. Test sera serially diluted in Blotto buffer were added to the assay plates for 1 h. After washing, the wells were incubated for 30 min in 1.5 M sodium thiocyanate (NaSCN; Sigma-Aldrich) or 1× phosphate-buffered saline (PBS) and washed again. HRP-conjugated goat anti-monkey Ab (KPL) was added at 1:1,000 and incubated for 1 h. The plates were washed as before and incubated in SureBlue TMB microwell peroxidase substrate (KPL) for 10 min. The reaction was stopped with 1 N H_2SO_4, and the plates were read on a spectrophotometer at 450 nm. The avidity index was calculated by taking the ratio of the NaSCN-treated plasma to the PBS-treated plasma.

Intracellular cytokine staining. Cryopreserved PBMCs were thawed in a 37°C water bath. The cells were then transferred to prewarmed R10 (RPMI 1640 [BioWhittaker, Walkersville, MD], 10% fetal bovine serum (FBS), 2 mM L-glutamine, 100 U/ml penicillin G, 100 μg/ml streptomycin) with 50 U/ml Benzonase (Novagen, Madison, WI) and washed. Cells were then resuspended at 1 million to 2 million cells/ml in R10

(RPMI 1640, 10% FBS, 1× Anti-Anti) and rested overnight in a 37°C/5% CO_2 incubator. The following morning, cells were stimulated at 1 million to 3 million cells/well in a 96-well v-bottom plate with peptide pools (final concentration of 2 μg/ml) in the presence of GolgiPlug (at a final concentration of 10 μg/ml; BD Biosciences, San Jose, CA) for 6 h. Negative controls received an equal concentration of dimethyl sulfoxide (DMSO) instead of peptides. At the end of the incubation, the plate was transferred to 4°C overnight.

Intracellular cytokine staining was performed as outlined (68). The following monoclonal antibodies were used: CD4-BV421 (clone OKT4; BioLegend), CD8-BV570 (clone RPA-T8; BioLegend), CD69-ECD (clone TP1.55.3; Beckman Coulter), CD3-Cy7APC (clone SP34.2; BD Biosciences), IFN-γ-APC (clone B27; BD Biosciences), IL-2-PE (clone MQ1-17H12; BD Biosciences), and TNF-FITC (clone Mab11; BD Biosciences). Aqua LIVE/DEAD kit (Invitrogen, Carlsbad, CA) was used to exclude dead cells. All antibodies were previously titrated to determine the optimal concentration. Samples were acquired on an LSR II flow cytometer and analyzed using FlowJo version 9.6.3 (TreeStar, Inc., Ashland, OR).

CD4$^+$ T cell staining in LNs. Cells from lymph nodes (LNs) collected at week 13 were stained with the following antibodies: PerCPCy5.5 anti-CD4, Ax700 anti-CD3, FITC anti-Ki67, and BV650 anti-CCR5 (3A9, 5 μl), all from BD Bioscience, and APC anti-$\alpha4\beta7$ provided by the NIH Nonhuman Primate Reagent Resource (R24 OD010976 and NIAID contract HHSN 272201300031C) to assess CD4$^+$ T cell activation. Gating was done on live CD3$^+$ CD4$^+$ cells, and the frequency of Ki67$^+$ and CCR5$^+$ cells was calculated on CD4$^+$ T cells. The frequency of $\alpha4\beta7$ and CD38 was calculated on Ki67$^+$ CD4$^+$ T cells. For T_{FH} cells staining, PE-eFluor 610 anti-CD185 (CXCR5) (MU5UBEE, number 61-9185-42, 5 μl; eBiocence), APC Cy7 anti-CXCR3 and APC anti-PD1 were used. T_{FH} cells were defined as CXCR5$^+$ PD1^{hi} CD4$^+$ T cells in peripheral LNs (40).

MDSC staining. Identification of MDSCs was performed as previously described (33). Briefly, PBMCs (5×10^6 to 10×10^6 cells) were stained with the following antibodies: CD3 (clone SP34-2; BD Biosciences; catalog number 563916, 1.0 μl) and CD20 (clone 2H7; BD Biosciences; catalog number 560735, 1.0 μl), both in PE-Cy7, and NHP-CD45-BV786 (clone D058-1283; BD Biosciences; catalog number 563861, 3.0 μl), CD14-APC (clone M5E2; BD Biosciences; catalog number 561390, 7.5 μl), CD16-FITC (clone 3G8; BD Biosciences; catalog number 555406, 5.0 μl), HLA-DR-APC-Cy7 (clone L243; BioLegend; catalog number 307618, 4.0 μl), CD11b-Pe-Cy5 (clone ICRF44; BioLegend; catalog number 301308, 0.0625 μl), CD192 (CCR2)-BV421 (clone 48607; BD Biosciences; catalog number 564067, 3.0 μl), and CD184 (CXCR4)-PE-CF594 (clone 12G5; BD Biosciences; catalog number 562389, 5.0 μl). Aqua LIVE/DEAD kit (Invitrogen; catalog number L34966, 3.0 μl) was used to exclude dead cells. For this identification panel, myeloid cells were gated as Lin$^-$ (CD3 & CD20) CD45$^+$ cells. MDSCs were identified as Lin$^-$ CD45$^+$ CD14$^+$ HLA-DR$^-$ in live cells. Flow cytometry acquisition was performed on an LSR II (BD Biosciences) with a minimum of 500,000 events recorded. Marker expression was examined using FACSDiva software (BD Biosciences) and further analyzed using FlowJo version 10.1 (TreeStar, Inc., Ashland, OR).

Kynurenine and tryptophan plasma levels. Tryptophan and kynurenine plasma concentrations were measured by using the tryptophan ELISA (Rocky Mountain Diagnostics, Colorado Springs, CO, USA; Catalog number BA E-2700) and kynurenine ELISA commercial kits (Rocky Mountain Diagnostics, Colorado Springs, CO, USA; catalog number BA E-2200). For tryptophan measurement, 20 μl of plasma were precipitated, the recovered supernatants were derivatized, and the product was used to perform the ELISA according to the manufacturer's instructions. For kynurenine assay, 10 μl of plasma were acylated and used to perform the ELISA according to the manufacturer's instructions. The data are presented as the ratio between kynurenine and tryptophan (Kyn/Tryp) levels.

Luminex. Cryopreserved peripheral blood mononuclear cells (PBMCs) or lymphoid cells isolated from lymph nodes were thawed in a 37°C water bath. The cells were then transferred in R10 medium (RPMI 1640, 10% FBS, 1× Anti-Anti), washed, and resuspended in R10 medium at 2 million cells/ml in a 96-well u-bottom plate. Cells were unstimulated or stimulated with env peptide pool (final concentration of 2 μg/ml) in the presence of purified mouse anti-human CD28 antibody at a final concentration of 0.5 μg/ml (BD Biosciences, San Jose, CA; catalog no. 556620) for 48 h. At the end of the incubation, the cells were pelleted by centrifuging at 1,000 × *g*, and supernatants were collected and stored at −80°C.

Cryopreserved supernatants were analyzed using three Milliplex nonhuman primate multiplex assays (EMD Millipore Corporation, Billerica, MA). The following targets were assayed following manufacturer instructions: IL-2, IL-4, IL-10, IFN-γ (catalog number PRCYTOMAG-40K-11), and IL-21 (catalog number PRCYT2MAG-40K-04). Plasma of 12 animals from the ALVAC group and 8 animals from the CD40L group were analyzed for soluble CD40L (Milliplex map kit, catalog number PRCYTOMAG-40K). Briefly, after thawing the samples in ice, 25 μl of each supernatant was loaded into the plate, and 25 μl of assay buffer and 25 μl of magnetic beads were added. The plates were incubated with agitation at 4°C for 18 h. At the end of the incubation, the plates were washed, and 25 μl of detection antibody were added to each well and incubated for 1 h at room temperature. Then, 25 μl of streptavidin-PE was added and incubated for 30 min at room temperature. Finally, wells were washed, 150 μl of sheath fluid was added, and samples were acquired on a Bio-Plex 200 system (Bio-Rad, Hercules, CA).

SIV viral load and CD4$^+$ T cell number. SIV_{mac251} in plasma was quantified by nucleic acid sequence-based amplification as previously described (69). SIV-DNA was quantified in mucosal tissues 3 weeks post SIV infection by a real-time quantitative PCR (qPCR) assay with sensitivity up to 10 copies/10^6 cells as previously described (70). CD4$^+$ T-cell counts were periodically determined from whole blood by flow cytometry as previously described (71).

Statistical analysis. The Mann-Whitney-Wilcoxon test for continuous factors was used to compare means of groups. A *P* value of <0.05 was considered evidence of a difference or trend, without correction for multiple comparisons except as noted. The Cochran-Armitage test was used for categorical data

analysis. Correlation analysis was performed using the Spearman rank correlation method with exact permutation *P* values calculated. The number of challenges before viral acquisition was assessed using the log rank test of the discrete-time proportional hazards model.

ACKNOWLEDGMENTS

This work was supported by the intramural U.S. National Cancer Institute (NCI) program. We acknowledge the following institutions for the grants supporting the authors: M. Ostrowski was supported by Canadian Institutes of Health Research (CIHR) grant THA-11906. Salary support for M. Ostrowski was provided by Ontario HIV Treatment Network (OHTN) grant AHRC G769. Contributions were made by the extramural NIAID program (grant HHSN27201100016C to X. Shen, G. D. Tomaras, and D. C. Montefiori), the Henry M. Jackson Foundation (HJF), the U.S. Department of Defense, and Collaboration for Aids Vaccine Discovery (CAVD) grants OPP1032325 (R. A. Koup) and OPP1147555 (R. A. Koup) from the Bill and Melinda Gates Foundation. H. V. Trinh and M. Rao were supported by a cooperative agreement (W81XWH-18-2-0040) between the Henry M. Jackson Foundation for the Advancement of Military Medicine, Inc., and the U.S. Department of Defense. H. V. Trinh was partially supported by a grant from the Swiss National Science Foundation (P3SMP3_148406/1).

The manuscript was reviewed by the Walter Reed Army Institute of Research. There is no objection to its presentation and/or publication. The views expressed are those of the authors and should not be construed to represent the positions of the U.S. Army, the Department of Defense, or HJF.

There is no competing financial interest.

The U.S. government in conjunction with Sanofi Pasteur holds patent 5766598, "Recombinant attenuated ALVAC canarypox virus expression vectors containing heterologous DNA segments encoding lentiviral gene," issued 16 June 1998 (72).

REFERENCES

1. Piot P, Abdool Karim SS, Hecht R, Legido-Quigley H, Buse K, Stover J, Resch S, Ryckman T, Mogedal S, Dybul M, Goosby E, Watts C, Kilonzo N, McManus J, Sidibe M, Commission U-L. 2015. Defeating AIDS–advancing global health. Lancet 386:171–218. https://doi.org/10.1016/S0140-6736(15)60658-4.
2. Fauci AS, Folkers GK, Marston HD. 2014. Ending the global HIV/AIDS pandemic: the critical role of an HIV vaccine. Clin Infect Dis 59(Suppl): S80–S84. https://doi.org/10.1093/cid/ciu420.
3. Rerks-Ngarm S, MOPH-TAVEG Investigators, Pitisuttithum P, Nitayaphan S, Kaewkungwal J, Chiu J, Paris R, Premsri N, Namwat C, de Souza M, Adams E, Benenson M, Gurunathan S, Tartaglia J, McNeil JG, Francis DP, Stablein D, Birx DL, Chunsuttiwat S, Khamboonruang C, Thongcharoen P, Robb ML, Michael NL, Kunasol P, Kim JH. 2009. Vaccination with ALVAC and AIDSVAX to prevent HIV-1 infection in Thailand. N Engl J Med 361:2209–2220. https://doi.org/10.1056/NEJMoa0908492.
4. Robb ML, Rerks-Ngarm S, Nitayaphan S, Pitisuttithum P, Kaewkungwal J, Kunasol P, Khamboonruang C, Thongcharoen P, Morgan P, Benenson M, Paris RM, Chiu J, Adams E, Francis D, Gurunathan S, Tartaglia J, Gilbert P, Stablein D, Michael NL, Kim JH. 2012. Risk behaviour and time as covariates for efficacy of the HIV vaccine regimen ALVAC-HIV (vCP1521) and AIDSVAX B/E: a post-hoc analysis of the Thai phase 3 efficacy trial RV 144. Lancet Infect Dis 12:531–537. https://doi.org/10.1016/S1473-3099(12)70088-9.
5. Haynes BF, Gilbert PB, McElrath MJ, Zolla-Pazner S, Tomaras GD, Alam SM, Evans DT, Montefiori DC, Karnasuta C, Sutthent R, Liao HX, DeVico AL, Lewis GK, Williams C, Pinter A, Fong Y, Janes H, DeCamp A, Huang Y, Rao M, Billings E, Karasavvas N, Robb ML, Ngauy V, de Souza MS, Paris R, Ferrari G, Bailer RT, Soderberg KA, Andrews C, Berman PW, Frahm N, De Rosa SC, Alpert MD, Yates NL, Shen X, Koup RA, Pitisuttithum P, Kaewkungwal J, Nitayaphan S, Rerks-Ngarm S, Michael NL, Kim JH. 2012. Immune-correlates analysis of an HIV-1 vaccine efficacy trial. N Engl J Med 366:1275–1286. https://doi.org/10.1056/NEJMoa1113425.
6. Karasavvas N, MOPH TAVEG Collaboration, Billings E, Rao M, Williams C, Zolla-Pazner S, Bailer RT, Koup RA, Madnote S, Arworn D, Shen X, Tomaras GD, Currier JR, Jiang M, Magaret C, Andrews C, Gottardo R, Gilbert P, Cardozo TJ, Rerks-Ngarm S, Nitayaphan S, Pitisuttithum P, Kaewkungwal J, Paris R, Greene K, Gao H, Gurunathan S, Tartaglia J, Sinangil F, Korber BT, Montefiori DC, Mascola JR, Robb ML, Haynes BF, Ngauy V, Michael NL, Kim JH, de Souza MS. 2012. The Thai phase III HIV type 1 vaccine trial (RV144) regimen induces antibodies that target conserved regions within the V2 loop of gp120. AIDS Res Hum Retroviruses 28:1444–1457. https://doi.org/10.1089/aid.2012.0103.
7. Yates NL, Liao H-X, Fong Y, deCamp A, Vandergrift NA, Williams WT, Alam SM, Ferrari G, Yang Z-Y, Seaton KE, Berman PW, Alpert MD, Evans DT, O'Connell RJ, Francis D, Sinangil F, Lee C, Nitayaphan S, Rerks-Ngarm S, Kaewkungwal J, Pitisuttithum P, Tartaglia J, Pinter A, Zolla-Pazner S, Gilbert PB, Nabel GJ, Michael NL, Kim JH, Montefiori DC, Haynes BF, Tomaras GD. 2014. Vaccine-induced Env V1-V2 IgG3 correlates with lower HIV-1 infection risk and declines soon after vaccination. Sci Transl Med 6:228ra39. https://doi.org/10.1126/scitranslmed.3007730.
8. Zolla-Pazner S, deCamp A, Gilbert PB, Williams C, Yates NL, Williams WT, Howington R, Fong Y, Morris DE, Soderberg KA, Irene C, Reichman C, Pinter A, Parks R, Pitisuttithum P, Kaewkungwal J, Rerks-Ngarm S, Nitayaphan S, Andrews C, O'Connell RJ, Yang Z-Y, Nabel GJ, Kim JH, Michael NL, Montefiori DC, Liao H-X, Haynes BF, Tomaras GD. 2014. Vaccine-induced IgG antibodies to V1V2 regions of multiple HIV-1 subtypes correlate with decreased risk of HIV-1 infection. PLoS One 9:e87572. https://doi.org/10.1371/journal.pone.0087572.
9. Montefiori DC, Karnasuta C, Huang Y, Ahmed H, Gilbert P, de Souza MS, McLinden R, Tovanabutra S, Laurence-Chenine A, Sanders-Buell E, Moody MA, Bonsignori M, Ochsenbauer C, Kappes J, Tang H, Greene K, Gao H, LaBranche CC, Andrews C, Polonis VR, Rerks-Ngarm S, Pitisuttithum P, Nitayaphan S, Kaewkungwal J, Self SG, Berman PW, Francis D, Sinangil F, Lee C, Tartaglia J, Robb ML, Haynes BF, Michael NL, Kim JH. 2012. Magnitude and breadth of the neutralizing antibody response in the RV144 and Vax003 HIV-1 vaccine efficacy trials. J Infect Dis 206: 431–441. https://doi.org/10.1093/infdis/jis367.
10. Gottardo R, Bailer RT, Korber BT, Gnanakaran S, Phillips J, Shen X, Tomaras GD, Turk E, Imholte G, Eckler L, Wenschuh H, Zerweck J, Greene K, Gao H, Berman PW, Francis D, Sinangil F, Lee C, Nitayaphan S, Rerks-Ngarm S, Kaewkungwal J, Pitisuttithum P, Tartaglia J, Robb ML, Michael NL, Kim JH, Zolla-Pazner S, Haynes BF, Mascola JR, Self S, Gilbert

P, Montefiori DC. 2013. Plasma IgG to linear epitopes in the V2 and V3 regions of HIV-1 gp120 correlate with a reduced risk of infection in the RV144 vaccine efficacy trial. PLoS One 8:e75665. https://doi.org/10.1371/journal.pone.0075665.
11. de Souza MS, Ratto-Kim S, Chuenarom W, Schuetz A, Chantakulkij S, Nuntapinit B, Valencia-Micolta A, Thelian D, Nitayaphan S, Pitisuttithum P, Paris RM, Kaewkungwal J, Michael NL, Rerks-Ngarm S, Mathieson B, Marovich M, Currier JR, Kim JH, Ministry of Public Health-Thai AVEGC. 2012. The Thai phase III trial (RV144) vaccine regimen induces T cell responses that preferentially target epitopes within the V2 region of HIV-1 envelope. J Immunol 188:5166–5176. https://doi.org/10.4049/jimmunol.1102756.
12. Lin L, Finak G, Ushey K, Seshadri C, Hawn TR, Frahm N, Scriba TJ, Mahomed H, Hanekom W, Bart P-A, Pantaleo G, Tomaras GD, Rerks-Ngarm S, Kaewkungwal J, Nitayaphan S, Pitisuttithum P, Michael NL, Kim JH, Robb ML, O'Connell RJ, Karasavvas N, Gilbert P, C De Rosa S, McElrath MJ, Gottardo R. 2015. COMPASS identifies T-cell subsets correlated with clinical outcomes. Nat Biotechnol 33:610–616. https://doi.org/10.1038/nbt.3187.
13. Kim JH, Excler JL, Michael NL. 2015. Lessons from the RV144 Thai phase III HIV-1 vaccine trial and the search for correlates of protection. Annu Rev Med 66:423–437. https://doi.org/10.1146/annurev-med-052912-123749.
14. Pegu P, Vaccari M, Gordon S, Keele BF, Doster M, Guan Y, Ferrari G, Pal R, Ferrari MG, Whitney S, Hudacik L, Billings E, Rao M, Montefiori D, Tomaras G, Alam SM, Fenizia C, Lifson JD, Stablein D, Tartaglia J, Michael N, Kim J, Venzon D, Franchini G. 2013. Antibodies with high avidity to the gp120 envelope protein in protection from simian immunodeficiency virus SIV(mac251) acquisition in an immunization regimen that mimics the RV-144 Thai trial. J Virol 87:1708–1719. https://doi.org/10.1128/JVI.02544-12.
15. Vaccari M, Gordon SN, Fourati S, Schifanella L, Liyanage NPM, Cameron M, Keele BF, Shen X, Tomaras GD, Billings E, Rao M, Chung AW, Dowell KG, Bailey-Kellogg C, Brown EP, Ackerman ME, Vargas-Inchaustegui DA, Whitney S, Doster MN, Binello N, Pegu P, Montefiori DC, Foulds K, Quinn DS, Donaldson M, Liang F, Loré K, Roederer M, Koup RA, McDermott A, Ma Z-M, Miller CJ, Phan TB, Forthal DN, Blackburn M, Caccuri F, Bissa M, Ferrari G, Kalyanaraman V, Ferrari MG, Thompson D, Robert-Guroff M, Ratto-Kim S, Kim JH, Michael NL, Phogat S, Barnett SW, Tartaglia J, Venzon D, Stablein DM, Alter G, Sekaly R-P, Franchini G. 2016. Adjuvant-dependent innate and adaptive immune signatures of risk of SIVmac251 acquisition. Nat Med 22:762–770. https://doi.org/10.1038/nm.4105.
16. Vaccari M, Keele BF, Bosinger SE, Doster MN, Ma Z-M, Pollara J, Hryniewicz A, Ferrari G, Guan Y, Forthal DN, Venzon D, Fenizia C, Morgan T, Montefiori D, Lifson JD, Miller CJ, Silvestri G, Rosati M, Felber BK, Pavlakis GN, Tartaglia J, Franchini G. 2013. Protection afforded by an HIV vaccine candidate in macaques depends on the dose of SIVmac251 at challenge exposure. J Virol 87:3538–3548. https://doi.org/10.1128/JVI.02863-12.
17. Vaccari M, Fourati S, Gordon SN, Brown DR, Bissa M, Schifanella L, Silva de Castro I, Doster MN, Galli V, Omsland M, Fujikawa D, Gorini G, Liyanage NPM, Trinh HV, McKinnon KM, Foulds KE, Keele BF, Roederer M, Koup RA, Shen X, Tomaras GD, Wong MP, Munoz KJ, Gach JS, Forthal DN, Montefiori DC, Venzon DJ, Felber BK, Rosati M, Pavlakis GN, Rao M, Sekaly R-P, Franchini G. 2018. HIV vaccine candidate activation of hypoxia and the inflammasome in CD14+ monocytes is associated with a decreased risk of SIVmac251 acquisition. Nat Med 24:847–856. https://doi.org/10.1038/s41591-018-0025-7.
18. Gordon SN, Liyanage NP, Doster MN, Vaccari M, Vargas-Inchaustegui DA, Pegu P, Schifanella L, Shen X, Tomaras GD, Rao M, Billings EA, Schwartz J, Prado I, Bobb K, Zhang W, Montefiori DC, Foulds KE, Ferrari G, Robert-Guroff M, Roederer M, Phan TB, Forthal DN, Stablein DM, Phogat S, Venzon DJ, Fouts T, Franchini G. 2016. Boosting of ALVAC-SIV vaccine-primed macaques with the CD4-SIVgp120 fusion protein elicits antibodies to V2 associated with a decreased risk of SIVmac251 acquisition. J Immunol 197:2726–2737. https://doi.org/10.4049/jimmunol.1600674.
19. Liu J, Ostrowski M. 2010. Development of TNFSF as molecular adjuvants for ALVAC HIV-1 vaccines. Hum Vaccin 6:355–359. https://doi.org/10.4161/hv.6.4.10867.
20. Elgueta R, Benson MJ, de Vries VC, Wasiuk A, Guo Y, Noelle RJ. 2009. Molecular mechanism and function of CD40/CD40L engagement in the immune system. Immunol Rev 229:152–172. https://doi.org/10.1111/j.1600-065X.2009.00782.x.
21. Bennett SR, Carbone FR, Karamalis F, Flavell RA, Miller JF, Heath WR. 1998. Help for cytotoxic-T-cell responses is mediated by CD40 signalling. Nature 393:478–480. https://doi.org/10.1038/30996.
22. Bishop GA, Hostager BS. 2001. Signaling by CD40 and its mimics in B cell activation. Immunol Res 24:97–109. https://doi.org/10.1385/IR:24:2:097.
23. Bishop GA, Hostager BS. 2003. The CD40-CD154 interaction in B cell-T cell liaisons. Cytokine Growth Factor Rev 14:297–309. https://doi.org/10.1016/s1359-6101(03)00024-8.
24. Liu J, Yu Q, Stone GW, Yue FY, Ngai N, Jones RB, Kornbluth RS, Ostrowski MA. 2008. CD40L expressed from the canarypox vector, ALVAC, can boost immunogenicity of HIV-1 canarypox vaccine in mice and enhance the in vitro expansion of viral specific CD8+ T cell memory responses from HIV-1-infected and HIV-1-uninfected individuals. Vaccine 26:4062–4072. https://doi.org/10.1016/j.vaccine.2008.05.018.
25. Lin FC, Peng Y, Jones LA, Verardi PH, Yilma TD. 2009. Incorporation of CD40 ligand into the envelope of pseudotyped single-cycle simian immunodeficiency viruses enhances immunogenicity. J Virol 83:1216–1227. https://doi.org/10.1128/JVI.01870-08.
26. Kwa S, Lai L, Gangadhara S, Siddiqui M, Pillai VB, Labranche C, Yu T, Moss B, Montefiori DC, Robinson HL, Kozlowski PA, Amara RR. 2014. CD40L-adjuvanted DNA/modified vaccinia virus Ankara simian immunodeficiency virus SIV239 vaccine enhances SIV-specific humoral and cellular immunity and improves protection against a heterologous SIVE660 mucosal challenge. J Virol 88:9579–9589. https://doi.org/10.1128/JVI.00975-14.
27. Kwa S, Sadagopal S, Shen X, Hong JJ, Gangadhara S, Basu R, Victor B, Iyer SS, LaBranche CC, Montefiori DC, Tomaras GD, Villinger F, Moss B, Kozlowski PA, Amara RR. 2015. CD40L-adjuvanted DNA/modified vaccinia virus Ankara simian immunodeficiency virus (SIV) vaccine enhances protection against neutralization-resistant mucosal SIV infection. J Virol 89:4690–4695. https://doi.org/10.1128/JVI.03527-14.
28. Stone GW, Barzee S, Snarsky V, Kee K, Spina CA, Yu XF, Kornbluth RS. 2006. Multimeric soluble CD40 ligand and GITR ligand as adjuvants for human immunodeficiency virus DNA vaccines. J Virol 80:1762–1772. https://doi.org/10.1128/JVI.80.4.1762-1772.2006.
29. Franco D, Liu W, Gardiner DF, Hahn BH, Ho DD. 2011. CD40L-containing virus-like particle as a candidate HIV-1 vaccine targeting dendritic cells. J Acquir Immune Defic Syndr 56:393–400. https://doi.org/10.1097/QAI.0b013e31820b844e.
30. Zhang R, Zhang S, Li M, Chen C, Yao Q. 2010. Incorporation of CD40 ligand into SHIV virus-like particles (VLP) enhances SHIV-VLP-induced dendritic cell activation and boosts immune responses against HIV. Vaccine 28:5114–5127. https://doi.org/10.1016/j.vaccine.2010.03.079.
31. Gomez CE, Najera JL, Sanchez R, Jimenez V, Esteban M. 2009. Multimeric soluble CD40 ligand (sCD40L) efficiently enhances HIV specific cellular immune responses during DNA prime and boost with attenuated poxvirus vectors MVA and NYVAC expressing HIV antigens. Vaccine 27:3165–3174. https://doi.org/10.1016/j.vaccine.2009.03.049.
32. Pal R, Venzon D, Letvin NL, Santra S, Montefiori DC, Miller NR, Tryniszewska E, Lewis MG, VanCott TC, Hirsch V, Woodward R, Gibson A, Grace M, Dobratz E, Markham PD, Hel Z, Nacsa J, Klein M, Tartaglia J, Franchini G. 2002. ALVAC-SIV-gag-pol-env-based vaccination and macaque major histocompatibility complex class I (A*01) delay simian immunodeficiency virus SIVmac-induced immunodeficiency. J Virol 76:292–302. https://doi.org/10.1128/jvi.76.1.292-302.2002.
33. Vaccari M, Fourati S, Brown DR, Silva de Castro I, Bissa M, Schifanella L, Doster MN, Foulds KE, Roederer M, Koup RA, Sui Y, Berzofsky JA, Sekaly RP, Franchini G. 2019. Myeloid cell crosstalk regulates the efficacy of the DNA/ALVAC/gp120 HIV vaccine candidate. Front Immunol 10:1072. https://doi.org/10.3389/fimmu.2019.01072.
34. Keele BF, Li H, Learn GH, Hraber P, Giorgi EE, Grayson T, Sun C, Chen Y, Yeh WW, Letvin NL, Mascola JR, Nabel GJ, Haynes BF, Bhattacharya T, Perelson AS, Korber BT, Hahn BH, Shaw GM. 2009. Low-dose rectal inoculation of rhesus macaques by SIVsmE660 or SIVmac251 recapitulates human mucosal infection by HIV-1. J Exp Med 206:1117–1134. https://doi.org/10.1084/jem.20082831.
35. Keele BF, Giorgi EE, Salazar-Gonzalez JF, Decker JM, Pham KT, Salazar MG, Sun C, Grayson T, Wang S, Li H, Wei X, Jiang C, Kirchherr JL, Gao F, Anderson JA, Ping LH, Swanstrom R, Tomaras GD, Blattner WA, Goepfert PA, Kilby JM, Saag MS, Delwart EL, Busch MP, Cohen MS, Montefiori DC, Haynes BF, Gaschen B, Athreya GS, Lee HY, Wood N, Seoighe C, Perelson AS, Bhattacharya T, Korber BT, Hahn BH, Shaw GM. 2008. Identification and characterization of transmitted and early founder virus envelopes in primary HIV-1 infection. Proc Natl Acad Sci U S A 105:7552–7557. https://doi.org/10.1073/pnas.0802203105.

36. van Kooten C, Banchereau J. 1997. Functional role of CD40 and its ligand. Int Arch Allergy Immunol 113:393–399. https://doi.org/10.1159/000237614.
37. Erickson LD, Durell BG, Vogel LA, O'Connor BP, Cascalho M, Yasui T, Kikutani H, Noelle RJ. 2002. Short-circuiting long-lived humoral immunity by the heightened engagement of CD40. J Clin Invest 109:613–620. https://doi.org/10.1172/JCI14110.
38. Yamamoto T, Lynch RM, Gautam R, Matus-Nicodemos R, Schmidt SD, Boswell KL, Darko S, Wong P, Sheng Z, Petrovas C, McDermott AB, Seder RA, Keele BF, Shapiro L, Douek DC, Nishimura Y, Mascola JR, Martin MA, Koup RA. 2015. Quality and quantity of T_{FH} cells are critical for broad antibody development in $SHIV_{AD8}$ infection. Sci Transl Med 7:298ra120. https://doi.org/10.1126/scitranslmed.aab3964.
39. Vaccari M, Franchini G. 2018. T cell subsets in the germinal center: lessons from the macaque model. Front Immunol 9:348. https://doi.org/10.3389/fimmu.2018.00348.
40. Blackburn MJ, Zhong-Min M, Caccuri F, McKinnon K, Schifanella L, Guan Y, Gorini G, Venzon D, Fenizia C, Binello N, Gordon SN, Miller CJ, Franchini G, Vaccari M. 2015. Regulatory and helper follicular T cells and antibody avidity to simian immunodeficiency virus glycoprotein 120. J Immunol 195:3227–3236. https://doi.org/10.4049/jimmunol.1402699.
41. Lin A, Liang F, Thompson EA, Vono M, Ols S, Lindgren G, Hassett K, Salter H, Ciaramella G, Lore K. 2018. Rhesus macaque myeloid-derived suppressor cells demonstrate T cell inhibitory functions and are transiently increased after vaccination. J Immunol 200:286–294. https://doi.org/10.4049/jimmunol.1701005.
42. Wang L, Zhao J, Ren JP, Wu XY, Morrison ZD, Elgazzar MA, Ning SB, Moorman JP, Yao ZQ. 2016. Expansion of myeloid-derived suppressor cells promotes differentiation of regulatory T cells in HIV-1+ individuals. AIDS 30:1521–1531. https://doi.org/10.1097/QAD.0000000000001083.
43. Filipazzi P, Huber V, Rivoltini L. 2012. Phenotype, function and clinical implications of myeloid-derived suppressor cells in cancer patients. Cancer Immunol Immunother 61:255–263. https://doi.org/10.1007/s00262-011-1161-9.
44. Schlom J, Jochems C, Gulley JL, Huang J. 2013. The role of soluble CD40L in immunosuppression. Oncoimmunology 2:e22546. https://doi.org/10.4161/onci.22546.
45. Jenabian MA, Patel M, Kema I, Vyboh K, Kanagaratham C, Radzioch D, Thebault P, Lapointe R, Gilmore N, Ancuta P, Tremblay C, Routy JP. 2014. Soluble CD40-ligand (sCD40L, sCD154) plays an immunosuppressive role via regulatory T cell expansion in HIV infection. Clin Exp Immunol 178:102–111. https://doi.org/10.1111/cei.12396.
46. Aukrust P, Muller F, Ueland T, Berget T, Aaser E, Brunsvig A, Solum NO, Forfang K, Froland SS, Gullestad L. 1999. Enhanced levels of soluble and membrane-bound CD40 ligand in patients with unstable angina. Possible reflection of T lymphocyte and platelet involvement in the pathogenesis of acute coronary syndromes. Circulation 100:614–620. https://doi.org/10.1161/01.cir.100.6.614.
47. Bretscher PA. 1999. A two-step, two-signal model for the primary activation of precursor helper T cells. Proc Natl Acad Sci U S A 96:185–190. https://doi.org/10.1073/pnas.96.1.185.
48. Zhang B, Wu T, Chen M, Zhou Y, Yi D, Guo R. 2013. The CD40/CD40L system: a new therapeutic target for disease. Immunol Lett 153:58–61. https://doi.org/10.1016/j.imlet.2013.07.005.
49. Kawabe T, Naka T, Yoshida K, Tanaka T, Fujiwara H, Suematsu S, Yoshida N, Kishimoto T, Kikutani H. 1994. The immune responses in CD40-deficient mice: impaired immunoglobulin class switching and germinal center formation. Immunity 1:167–178. https://doi.org/10.1016/1074-7613(94)90095-7.
50. Chung AW, Ghebremichael M, Robinson H, Brown E, Choi I, Lane S, Dugast AS, Schoen MK, Rolland M, Suscovich TJ, Mahan AE, Liao L, Streeck H, Andrews C, Rerks-Ngarm S, Nitayaphan S, de Souza MS, Kaewkungwal J, Pitisuttithum P, Francis D, Michael NL, Kim JH, Bailey-Kellogg C, Ackerman ME, Alter G. 2014. Polyfunctional Fc-effector profiles mediated by IgG subclass selection distinguish RV144 and VAX003 vaccines. Sci Transl Med 6:228ra38. https://doi.org/10.1126/scitranslmed.3007736.
51. Vonderheide RH. 2007. Prospect of targeting the CD40 pathway for cancer therapy. Clin Cancer Res 13:1083–1088. https://doi.org/10.1158/1078-0432.CCR-06-1893.
52. Cella M, Scheidegger D, Palmer-Lehmann K, Lane P, Lanzavecchia A, Alber G. 1996. Ligation of CD40 on dendritic cells triggers production of high levels of interleukin-12 and enhances T cell stimulatory capacity: T-T help via APC activation. J Exp Med 184:747–752. https://doi.org/10.1084/jem.184.2.747.
53. Teigler JE, Phogat S, Franchini G, Hirsch VM, Michael NL, Barouch DH. 2014. The canarypox virus vector ALVAC induces distinct cytokine responses compared to the vaccinia virus-based vectors MVA and NYVAC in rhesus monkeys. J Virol 88:1809-14. https://doi.org/10.1128/JVI.02386-13.
54. Blair PJ, Riley JL, Harlan DM, Abe R, Tadaki DK, Hoffmann SC, White L, Francomano T, Perfetto SJ, Kirk AD, June CH. 2000. CD40 ligand (CD154) triggers a short-term CD4(+) T cell activation response that results in secretion of immunomodulatory cytokines and apoptosis. J Exp Med 191:651–660. https://doi.org/10.1084/jem.191.4.651.
55. Miller JF, Mitchell GF. 1968. Cell to cell interaction in the immune response. I. Hemolysin-forming cells in neonatally thymectomized mice reconstituted with thymus or thoracic duct lymphocytes. J Exp Med 128:801–820. https://doi.org/10.1084/jem.128.4.801.
56. Del Prete GQ, Scarlotta M, Newman L, Reid C, Parodi LM, Roser JD, Oswald K, Marx PA, Miller CJ, Desrosiers RC, Barouch DH, Pal R, Piatak M, Chertova E, Giavedoni LD, O'Connor DH, Lifson JD, Keele BF. 2013. Comparative characterization of transfection- and infection-derived simian immunodeficiency virus challenge stocks for in vivo nonhuman primate studies. J Virol 87:4584–4595. https://doi.org/10.1128/JVI.03507-12.
57. Cox WI, Tartaglia J, Paoletti E. 1993. Induction of cytotoxic T lymphocytes by recombinant canarypox (ALVAC) and attenuated vaccinia (NYVAC) viruses expressing the HIV-1 envelope glycoprotein. Virology 195:845–850. https://doi.org/10.1006/viro.1993.1442.
58. Taylor J, Trimarchi C, Weinberg R, Languet B, Guillemin F, Desmettre P, Paoletti E. 1991. Efficacy studies on a canarypox-rabies recombinant virus. Vaccine 9:190–193. https://doi.org/10.1016/0264-410x(91)90152-v.
59. Garcia-Arriaza J, Perdiguero B, Heeney J, Seaman M, Montefiori DC, Labranche C, Yates NL, Shen X, Tomaras GD, Ferrari G, Foulds KE, McDermott A, Kao SF, Roederer M, Hawkins N, Self S, Yao J, Farrell P, Phogat S, Tartaglia J, Barnett SW, Burke B, Cristillo A, Weiss D, Lee C, Kibler K, Jacobs B, Asbach B, Wagner R, Ding S, Pantaleo G, Esteban M. 2015. Head-to-head comparison of poxvirus NYVAC and ALVAC vectors expressing identical HIV-1 clade C immunogens in prime-boost combination with Env protein in nonhuman primates. J Virol 89:8525–8539. https://doi.org/10.1128/JVI.01265-15.
60. Goebel SJ, Johnson GP, Perkus ME, Davis SW, Winslow JP, Paoletti E. 1990. The complete DNA sequence of vaccinia virus. Virology 179:247–266. https://doi.org/10.1016/0042-6822(90)90294-2.
61. Kent KA, Gritz L, Stallard G, Cranage MP, Collignon C, Thiriart C, Corcoran T, Silvera P, Stott EJ. 1991. Production and of monoclonal antibodies to simian immunodeficiency virus envelope glycoproteins. AIDS 5:829–836. https://doi.org/10.1097/00002030-199107000-00006.
62. Kent KA, Rud E, Corcoran T, Powell C, Thiriart C, Collignon C, Stott EJ. 1992. Identification of two neutralizing and 8 non-neutralizing epitopes on simian immunodeficiency virus envelope using monoclonal antibodies. AIDS Res Hum Retroviruses 8:1147–1151. https://doi.org/10.1089/aid.1992.8.1147.
63. Strbo N, Vaccari M, Pahwa S, Kolber MA, Doster MN, Fisher E, Gonzalez L, Stablein D, Franchini G, Podack ER. 2013. Cutting edge: novel vaccination modality provides significant protection against mucosal infection by highly pathogenic simian immunodeficiency virus. J Immunol 190:2495–2499. https://doi.org/10.4049/jimmunol.1202655.
64. Tomaras GD, Yates NL, Liu P, Qin L, Fouda GG, Chavez LL, Decamp AC, Parks RJ, Ashley VC, Lucas JT, Cohen M, Eron J, Hicks CB, Liao HX, Self SG, Landucci G, Forthal DN, Weinhold KJ, Keele BF, Hahn BH, Greenberg ML, Morris L, Karim SS, Blattner WA, Montefiori DC, Shaw GM, Perelson AS, Haynes BF. 2008. Initial B-cell responses to transmitted human immunodeficiency virus type 1: virion-binding immunoglobulin M (IgM) and IgG antibodies followed by plasma anti-gp41 antibodies with ineffective control of initial viremia. J Virol 82:12449–12463. https://doi.org/10.1128/JVI.01708-08.
65. Montefiori DC. 2005. Evaluating neutralizing antibodies against HIV, SIV, and SHIV in luciferase reporter gene assays. Curr Protoc Immunol Chapter 12:12.11. https://doi.org/10.1002/0471142735.im1211s64.
66. Schiffner T, Kong L, Duncan CJ, Back JW, Benschop JJ, Shen X, Huang PS, Stewart-Jones GB, DeStefano J, Seaman MS, Tomaras GD, Montefiori DC, Schief WR, Sattentau QJ. 2013. Immune focusing and enhanced neutralization induced by HIV-1 gp140 chemical cross-linking. J Virol 87:10163–10172. https://doi.org/10.1128/JVI.01161-13.
67. Li M, Gao F, Mascola JR, Stamatatos L, Polonis VR, Koutsoukos M, Voss G,

Goepfert P, Gilbert P, Greene KM, Bilska M, Kothe DL, Salazar-Gonzalez JF, Wei X, Decker JM, Hahn BH, Montefiori DC. 2005. Human immunodeficiency virus type 1 env clones from acute and early subtype B infections for standardized assessments of vaccine-elicited neutralizing antibodies. J Virol 79:10108–10125. https://doi.org/10.1128/JVI.79.16.10108-10125.2005.

68. Foulds KE, Donaldson M, Roederer M. 2012. OMIP-005: quality and phenotype of antigen-responsive rhesus macaque T cells. Cytometry A 81:360–361. https://doi.org/10.1002/cyto.a.22008.
69. Romano JW, Williams KG, Shurtliff RN, Ginocchio C, Kaplan M. 1997. NASBA technology: isothermal RNA amplification in qualitative and quantitative diagnostics. Immunol Invest 26:15–28. https://doi.org/10.3109/08820139709048912.
70. Lee EM, Chung HK, Livesay J, Suschak J, Finke L, Hudacik L, Galmin L, Bowen B, Markham P, Cristillo A, Pal R. 2010. Molecular methods for evaluation of virological status of nonhuman primates challenged with simian immunodeficiency or simian-human immunodeficiency viruses. J Virol Methods 163:287–294. https://doi.org/10.1016/j.jviromet.2009.10.012.
71. Vaccari M, Trindade CJ, Venzon D, Zanetti M, Franchini G. 2005. Vaccine-induced CD8+ central memory T cells in protection from simian AIDS. J Immunol 175:3502–3507. https://doi.org/10.4049/jimmunol.175.6.3502.
72. U.S. Government, Sanofi Pasteur. 16 June 1998. Recombinant attenuated ALVAC canarypox virus expression vectors containing heterologous DNA segments encoding lentiviral gene. US patent 5766598.